



GEOLOGICAL SURVEY OF CANADA

OPEN FILE 7408

**Portable XRF spectrometry of surficial sediments, NTS
75-I, 75-J, 75-O, 75-P (Mary Frances Lake – Whitefish
Lake – Thelon River area), Northwest Territories**

**A.P. Plourde, R.D. Knight, B.A. Kjarsgaard,
D.R. Sharpe, J-E. Lesemann**

2013



Natural Resources
Canada

Ressources naturelles
Canada

Canada



GEOLOGICAL SURVEY OF CANADA

OPEN FILE 7408

**Portable XRF spectrometry of surficial sediments,
NTS 75-I, 75-J, 75-O, 75-P (Mary Frances Lake –
Whitefish Lake – Thelon River area),
Northwest Territories**

A.P. Plourde, R.D. Knight, B.A. Kjarsgaard, D.R. Sharpe, J-E.. Lesemann

2013

©Her Majesty the Queen in Right of Canada 2013

doi:10.4095/292714

This publication is available for free download through GEOSCAN
(<http://geoscan.ess.nrcan.gc.ca/>).

Recommended citation

Plourde, A.P., Knight, R.D., Kjarsgaard, B.A., Sharpe, D.R. and Lesemann, J-E., 2013. Portable XRF spectrometry of surficial sediments, NTS 75-I, 75-J, 75-O, 75-P (Mary Frances Lake – Whitefish Lake – Thelon River area), Northwest Territories; Geological Survey of Canada, Open File 7408.
doi:10.4095/292714

Publications in this series have not been edited; they are released as submitted by the author.

Introduction

Portable X-ray fluorescence (pXRF) spectrometry is widely used due to its low-cost and rapid turn around for results, but questions persist regarding its accuracy, precision, comparison to traditional laboratory geochemical methods, and how the spectrometer is affected by field procedures. This study addresses some of these knowledge gaps by examining in-field pXRF methodologies and by comparing the results to laboratory analyses.

This report presents elemental concentrations, determined by pXRF spectrometry, of surficial sediment diamicton (till) and esker (sand) samples, collected in summer 2012. The study area encompasses parts of NTS map sheets 75-I, 75-J, 75-O, and 75-P; it covers approximately 3500 km², lying southwest of the Thelon Wildlife Sanctuary, and east of the area of interest for Thaidene Nene (Fig. 1). For this study, two sets of pXRF analyses were completed: one on the unprocessed field samples, and another after drying and sieving to <2 mm. Portable XRF spectrometry data from till samples are compared to ICP-MS/ES geochemical data (Kjarsgaard et al., 2013), in order to determine if pXRF can provide results comparable to those from laboratory geochemical methods. Results indicate that this tool can be used to guide sampling or follow-up sampling while in the field, and to assess samples for post-fieldwork laboratory based analyses.

Existing studies comparing pXRF to other geochemical analytical methods have shown the usefulness of the pXRF tool. In a study comparing pXRF data of sieved and unprocessed diamicton (till) collected from a borehole core, results indicate greater precision on the sieved sample compared to analysing the pebble-rich core directly (Plourde et al., 2012). Furthermore, Knight et al. (2012) compared pXRF to ICP-MS/ES (lithium borate fusion digestion) results for the <0.063 mm size fraction of a Champlain Sea (mud) aquitard. They concluded that for many elements pXRF results were comparable to the traditional geochemical methods and can be used to define the chemostratigraphy of silt- and clay-rich sediments.

Sample design and collection protocol

A total of 106 diamicton (till) and 65 esker (sand) samples of approximately 15 kg each were collected for heavy mineral analysis (Knight et al., in prep). Diamicton samples were collected based on a 10 km x 10 km grid, representing approximately one sample per 100 km². Eskers samples were collected at approximately 10 km intervals along each esker ridge crest. The distribution of sample sites is displayed in Figure 2. This sampling protocol replicates that used for the Thaidene Nene Mineral and Energy Resource Assessment (MERA) study (Kjarsgaard et al., 2013b) to the east of the present study area to provide a continuous data set. At each site a small (~30 mL plastic vial) sub-sample of sediment was collected for pXRF analyses. For each diamicton site, an additional 1 kg sample was collected. These samples were sent directly to Acme Analytical Laboratories Ltd. in Vancouver, BC for processing and geochemical analyses (Kjarsgaard et al.,

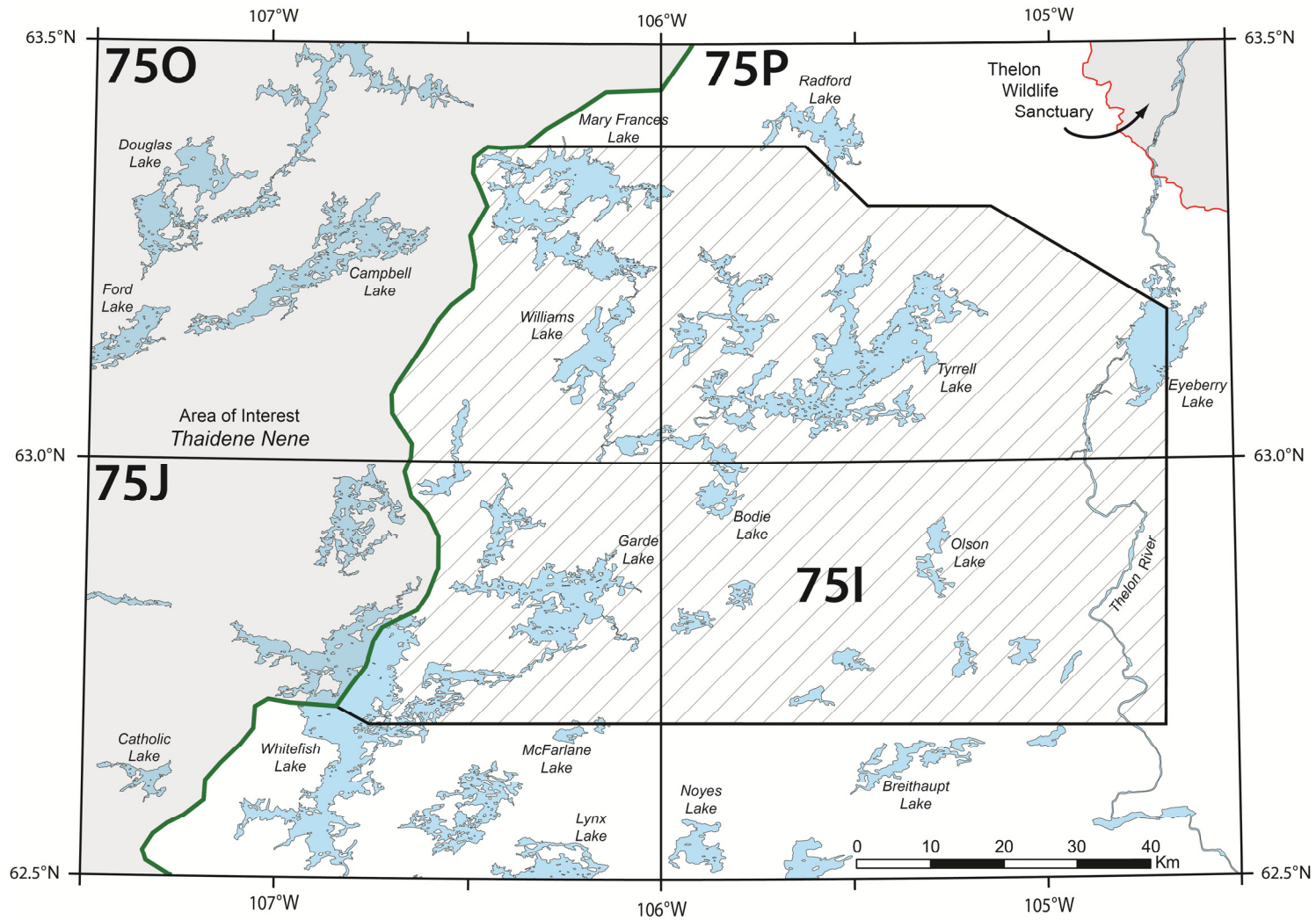


Figure 1. Location of the study area lying, southwest of the Thelon Wildlife Sanctuary and east of the area of interest for Thaidene Nene are shown for reference.

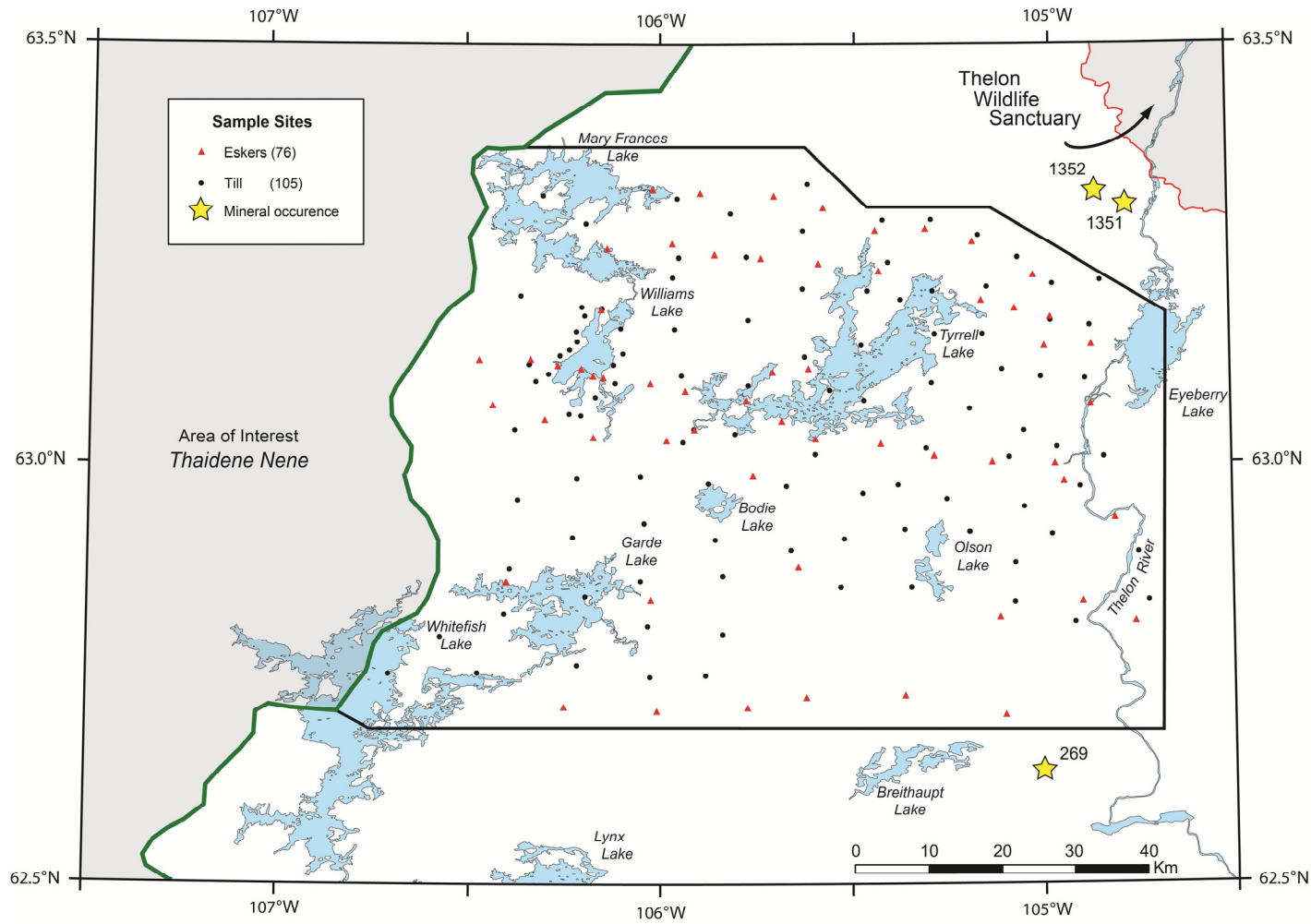


Figure 2. Distribution of till and esker sample sites and locations of known mineral occurrences within the study area. The Thelon Wildlife Sanctuary, and the area of interest for *Thaidene Nene* are shown for reference.

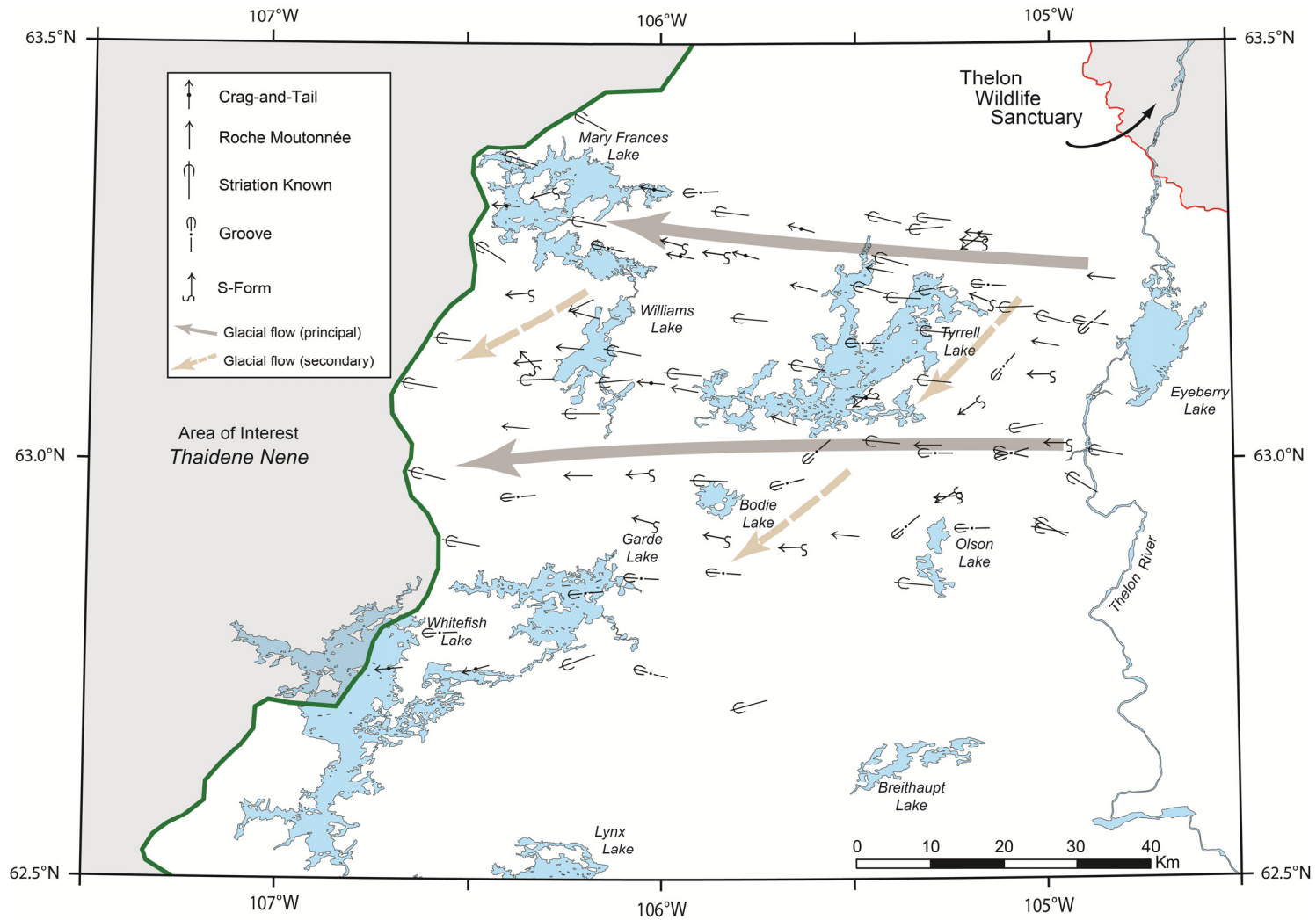


Figure 3. Glacial striae, groove, crag-and-tail, roche moutonnée and S-form data, with generalized flow direction.

2013a). When bedrock was present, paleoflow indicators (striations, s-forms, etc.) were measured (Fig. 3). For context, photographs were taken of each sample site and its relevant terrain conditions. A Trimble Yuma, with a modified Ganfeld field data capturing software, was used to digitally record standardised information about each sample and site, including GPS coordinates.

Methods

Due to the high cost of accessing each site by helicopter, it was decided that using the pXRF spectrometer directly in the field would not be cost effective, as it would add an additional 5-10 minutes of ground time for each sample analyzed. However, collecting a ~30 mL sample of sediment in a plastic vial required only seconds. Therefore the vial collected samples were analyzed each evening at the field camp. In addition, and perhaps more importantly, pXRF analysis in a the test stand at the field camp ensured that optimal sample – spectrometer geometry was maintained during the analysis, which may not be the case for an actual in-situ field analysis.

A handheld Thermo Scientific Niton XL3t GOLDD XRF spectrometer mounted in a test stand (Fig. 4) was used for this study. It is equipped with a Cygnit 50 keV 2 W silver anode X-ray tube, and a XL3 silicon drift detector (SDD) detector with 180,000 counts per second throughput. All analyses were carried out in Soil Mode where the expected elemental concentrations are <1%.



Figure 4. Placing a sample in the Niton pXRF test stand. The pXRF is being operated remotely by the yellow and black coloured Trimble Yuma.

A dwell time of 60 seconds was used for each of the Main (50 keV @ 40 μ A max), Low (20 keV @ 100 μ A max), and High (50 keV @ 40 μ A max) filters. After analysis the samples were placed in polystyrene anti-static weighing dishes (Fig. 5) and dried in a Thermo Scientific digitally temperature controlled oven at 60°C for approximately one hour. The sediment displayed in Figure 5 has not been dried and contains pebbles that are often not visible due to moist sand-silt adhering to the pebble surface. Figure 6 displays pebbles (>2mm) recovered after drying and sieving from approximately 100 till samples. The size and abundance of pebbles in what were originally perceived to be relatively pebble-free samples can be problematic with respect to obtaining accurate pXRF results, as previously described by Plourde et al., (2012) for a pebbly diamicton core. After drying, the samples were sieved to <2 mm, and re-analysed at the field camp using the same pXRF spectrometer and dwell times. For both pXRF analyses, a 4 μ m thick Prolene[®] film separated the sample from the detector (Fig. 7).



Figure 5. Sediment in polystyrene weighing dishes prior to drying. These samples contain pebbles that are not visible due to moisture adhesion of sediment. The weigh pans are 14 cm wide.



Figure 6. Size and abundance of pebbles recovered from approximately 100 samples after drying at 60°C for approximately one hour and sieving to <2mm. Note the large range in pebble sizes (all >2mm). The weigh pans are 14 cm wide.

For comparison of accuracy, two standard reference materials (Till-1 and Till-4) were analysed at the beginning and end of each session, as well as after every ~10 analyses. These reference materials are described by Lynch (1996), and results of a detailed pXRF study on these materials can be found in Knight et al. (2013). A SiO₂ blank was also analysed with the reference materials in order to ensure the test stand was not contaminated.

At Acme Laboratories Ltd., dried diamicton samples were sieved to <0.063 mm, then divided into three subsets. Each subset was analysed by ICP-MS/ES after three different digestion methods: aqua regia (partial digestion), 4-acid (near-total digestion), and lithium borate fusion (total digestion). More detailed descriptions of the analytical methods, as well as the data sets and their interpretation are provided in Kjarsgaard et al., (2013).

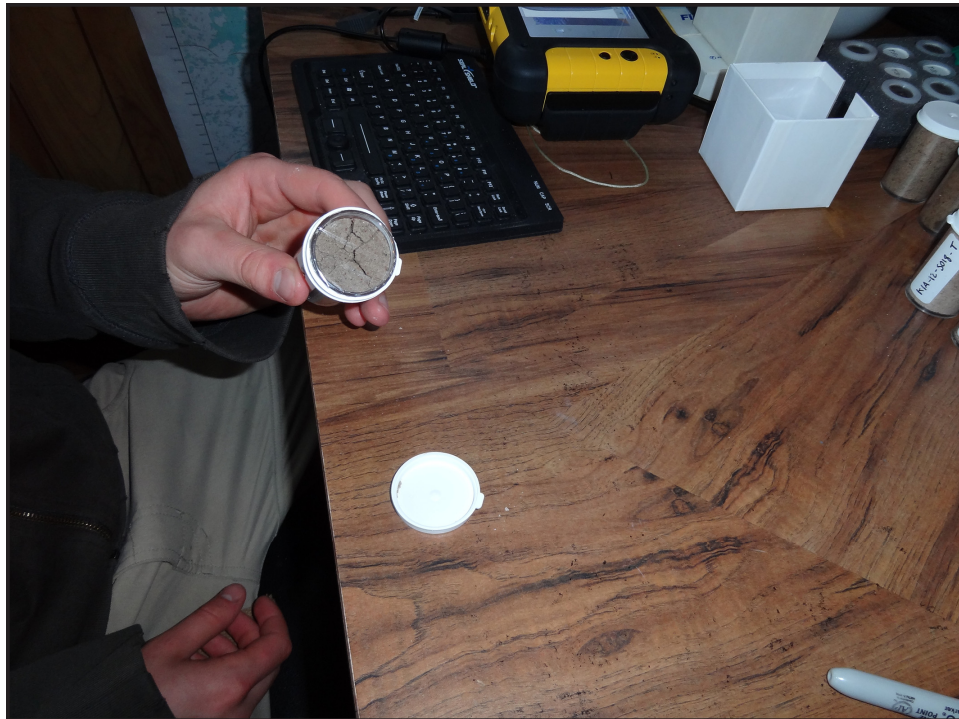


Figure 7. Sediment sample in a ~30 mL vial with 4 µm thick Prolene® film forming a seal to separate the sample from the detector.

Geology and geochemistry of the study area

The bedrock geology of the study area is dominated by Archean gneiss, granite and undifferentiated migmatite that are part of the Rae Domain of the Churchill Province (Fig. 8). At the eastern edge of the study area the Archean rocks are overlain by quartz sandstones of the Barrenlands Group within the Thelon Basin (Fig. 8; Kjarsgaard et al., 2013; Pehrsson et al., in press).

The surficial sediments in the study area lie within the Keewatin Sector of the former Laurentide Ice Sheet (LIS) west of the Keewatin Ice Divide (KID) (Lee et al., 1957; Lee, 1959). Terrain is of low relief and consists of flat plains to rolling hills. Glacial landforms such as eskers, transverse ridges, and various types of streamlined landforms (Fig. 9) form a roughly concentric zoned pattern around the former KID (Aylsworth and Shilts, 1989a, b). Consequently, the terrain is regionally streamlined in an east to west orientation, parallel to regional flow from the KID west to Great Slave Lake (Prest et al., 1968; Shaw et al., 2010). In the study area, sand and gravel are primary constituents of the till, occurring within streamlined landforms, within eskers, and forming a regional till cover of thickness ranging from ~1-50 m, but most commonly between 1-6 m thick. Barrenlands Group sandstones outcropping immediately east (up-ice-flow; Fig. 2) of the study area provide sand-sized quartz- and feldspar-rich sources, which account for the high levels of SiO₂ in the surficial sediments (Fig. 10); the surficial sediment contains correspondingly low amounts of most trace elements (Kjarsgaard et al., 2013). Additional details of the bedrock and surficial geology are presented by Kjarsgaard et al. (2013).

Results

Elemental concentrations determined by pXRF spectrometry are listed in Appendix A. The data are subdivided into three sample sets: (1) original unprocessed sample; (2) dried and sieved to <2 mm, and; (3) standard reference materials. Bivariate scatterplots comparing pXRF analyses of original field sample to dried and sieved <2 mm sample are displayed in Figure 11, for Ba, Ca, Fe, K, Mn, Ni, Pb, Rb, Sr, Ti, V, and Zr. In general, element concentrations are higher for the dried and sieved samples as compared to the original sediment sample. However, some elements such as Ba and to a lesser degree Sr display a higher concentration for the original sediment compared to the dried and sieved sediment (Fig. 11). Interpolated element concentration maps depicting the till geochemistry data were generated utilizing a Natural Neighbour interpolation methodology (MapInfo® Vertical Mapper software); the interpolation used a cell size of 100 m, an aggregation distance of 500 m, and a fixed colour profile for the 0th, 50th, 95th, 98th, and 100th percentiles. Interpolated maps for Cr, Cu, and Zn, were created in addition to the 12 elements plotted in Figure 11.

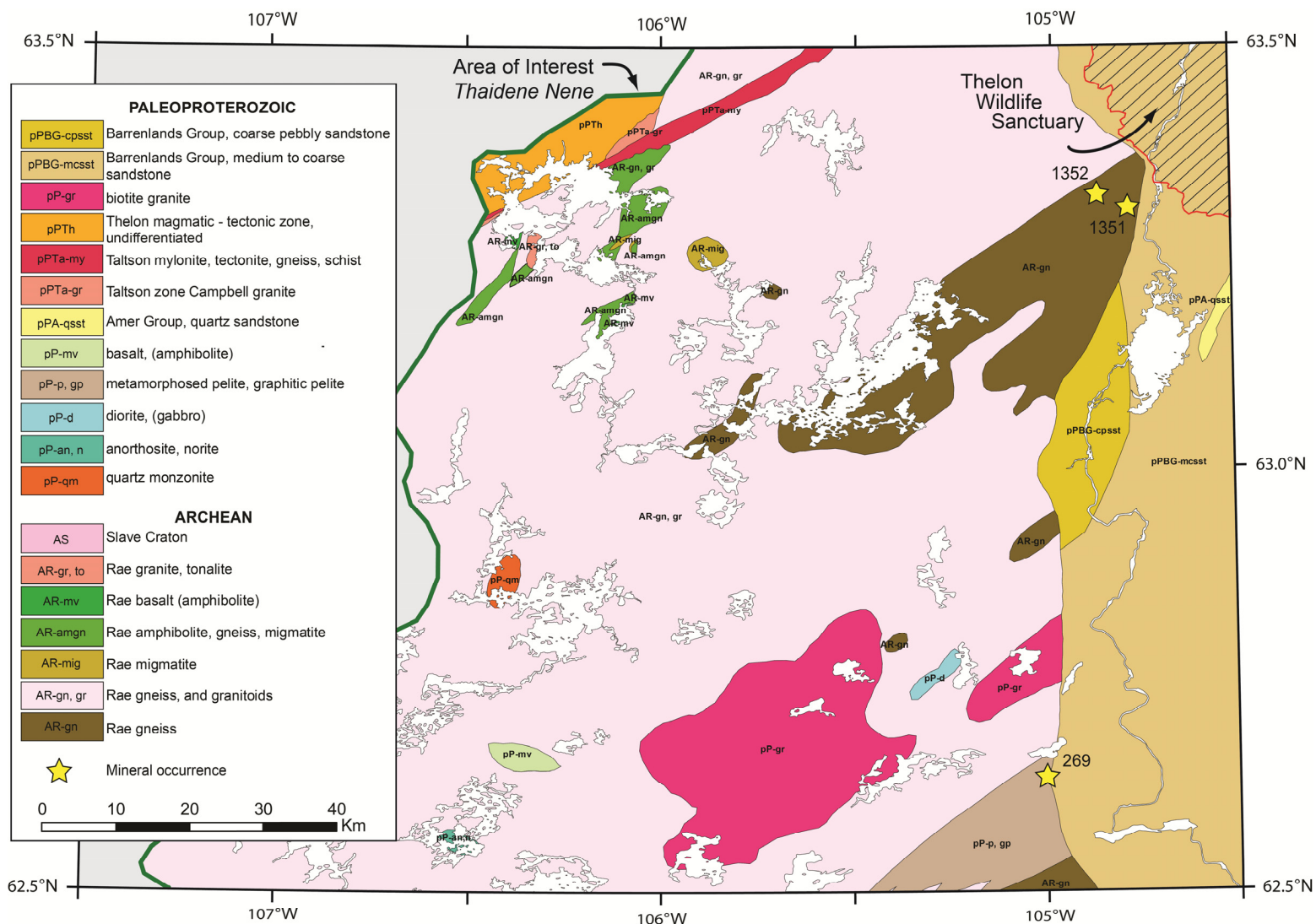


Figure 8. Bedrock geology map (1: 1 000 000 scale), with mineral showings. The west half of this map is from Kjarsgaard et al. (2013b, in press); east half of this map modified after Pehrsson et al. (2013, in press). Data source for mineral occurrences from NORMIN.DB (2011).

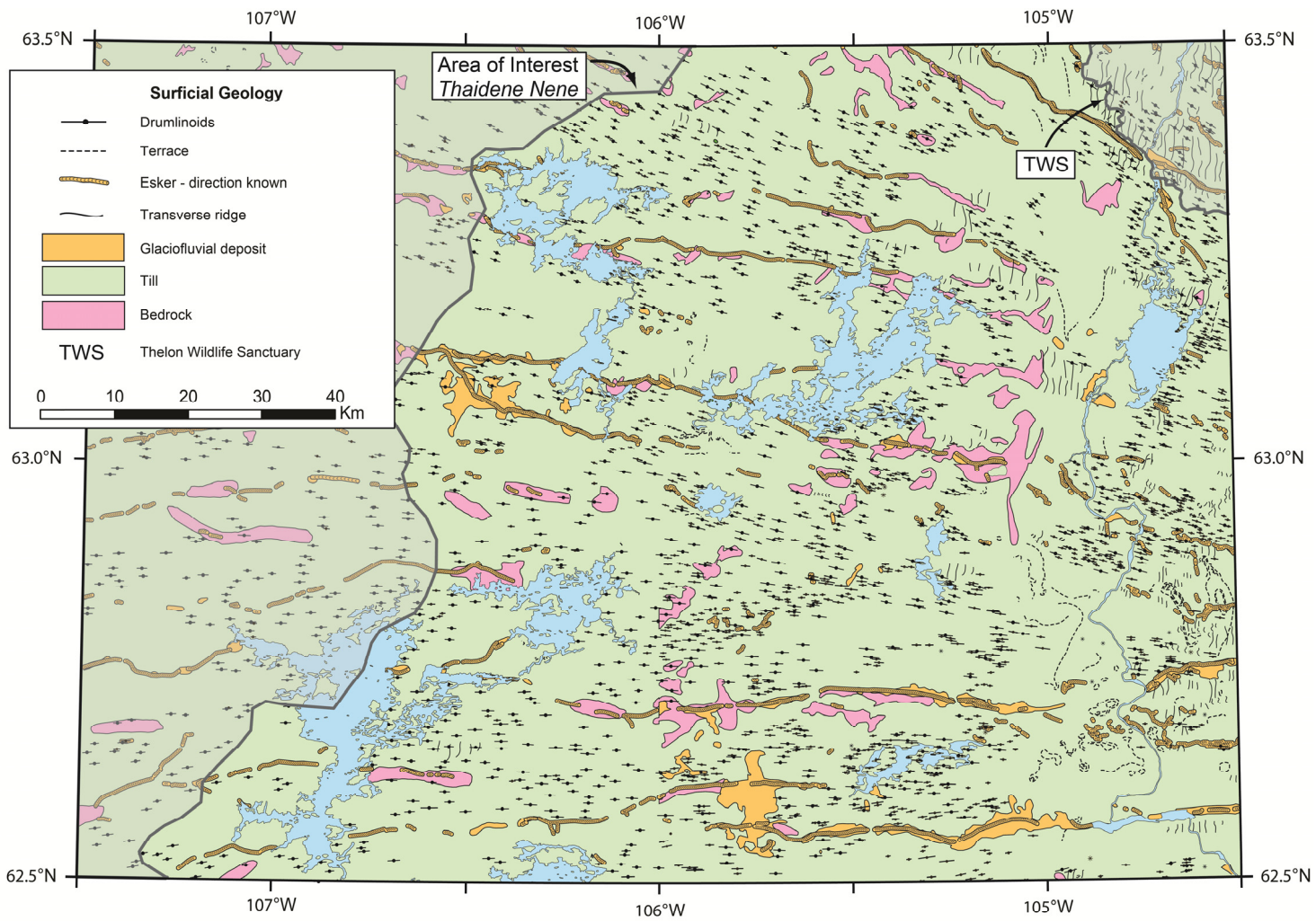


Figure 9. Simplified surficial geology, modified and updated from Craig, (1964) and Aylsworth and Shilts, (1989b).

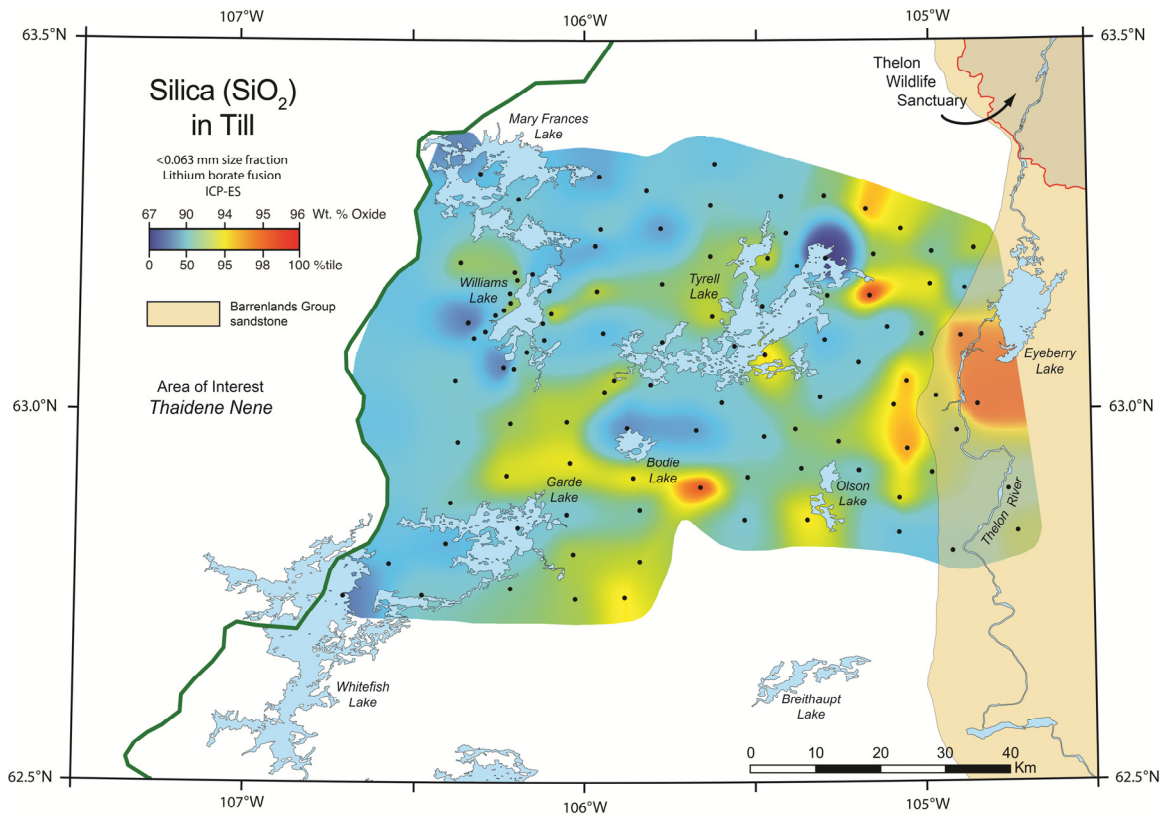


Figure 10. Weight % SiO₂ in till, as determined by ICP-ES following lithium borate fusion. Till sample sites are represented by black dots.

Till geochemistry maps generated from the dried and sieved <2mm fraction pXRF data are compared to those generated from, <0.063 mm (silt + clay) aqua regia, 4-acid, and lithium borate fusion data sets in Appendix B (data from Kjarsgaard et al., 2013). Figures 12 to 16 display maps for Cr, Cu, Fe, Rb, and Zn, respectively. Additional geochemical maps were produced using pXRF data from dry, <2 mm samples of till and eskers, for the same 15 elements, and are found in Appendix C; Figures 17 and 18 compare element maps produced by pXRF analyses of till and eskers, to only till analyses, for Pb and Ni, respectively.

Regionally interpolated maps using pXRF derived data reflect similar trends to maps generated using traditional laboratory based geochemistry methods.

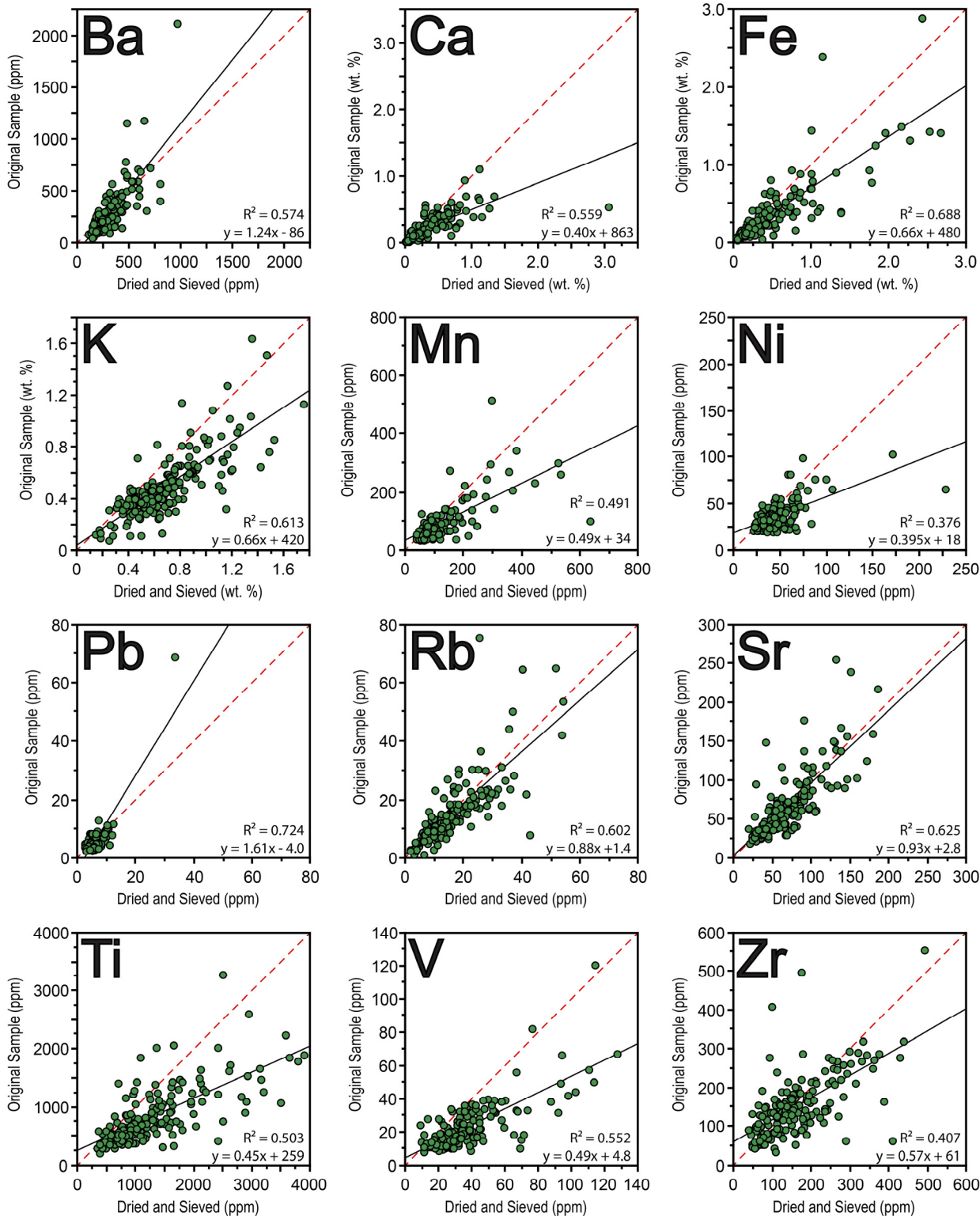


Figure 11. Comparison of pXRF analyses on the original unprocessed sample and the dried and sieved (<2 mm) subsample. Red dashed line represents the 1:1 ratio.

Discussion

A comparison of pXRF data obtained from the original unprocessed sample to that of the dried and sieved (<2 mm) sample is displayed in Figure 11, for each element that was consistently detected by the pXRF spectrometer. Coefficients of determination (r^2) range from 0.4 to 0.7. These somewhat weak correlations were in fact expected and are attributed to the effect of pebbles in the sediment prior to sieving, as seen in Figures 5 and 6. With the exceptions of Ba and Pb, slopes are all <1; most elements display higher elemental concentrations in the dried and sieved sample than the original unprocessed sample.

When the pXRF data is interpolated over the study area, it can be demonstrated that the data provides a reasonable reproduction of many of the geochemical maps constructed using the laboratory analysis ICP-MS/ES fusion results (Figs. 12 to 16). For most elements, the regional trends - typically higher concentrations in the west, lower in the east - are as evident in the maps generated with pXRF data as those made using traditional laboratory methods. Interpolated maps of Cr (Fig. 12) and Cu (Fig. 13), demonstrate that very strong geochemical anomalies (>10 times the mean) are reproducible with a pXRF spectrometer, despite the fact that most pXRF analyses were below the spectrometer's limit of detection (<LOD). More modest geochemical anomalies (3-10 times the mean) were also shown to be reproducible with pXRF spectrometry, however some were missed (e.g., Fig. 14, the Fe anomaly area immediately west of Williams Lake). In addition, some geochemical anomalies recognized in the pXRF data that are not observed in the laboratory data (e.g., Fig. 15, the moderate Rb anomaly at the northwest corner of the study area, and Fig. 16, the moderate Zn anomaly at the west edge of the study area). Some of these differences may be attributed to imprecision of the pXRF spectrometer, however the different size fractions analysed were likely a more important factor. Only the clay and silt size fractions (<0.063 mm) were used for the laboratory analyses, whereas the clay, silt, and sand size fractions (<2 mm) were used for pXRF analyses in the field.

Maps generated using both till and esker pXRF analyses demonstrate that, particularly in the northwest portion of the study area, some trace elements are more concentrated in the <2 mm size fraction of eskers than that of the surrounding till. For example, Ni in till has a maximum value of 75 ppm, whereas for the esker samples, the maximum value is 199 ppm (Fig. 17). High Ni values in esker samples are observed east and west of Williams Lake, and between Mary Frances and Tyrell Lakes. In contrast, Pb values in till and esker samples show similar maximum values of 32-33 ppm (Fig. 18). Mapping till and esker data together contrasts the two sediments, and as a result, makes regional (east-west) trends and true anomalies in the diamicton less obvious. While the esker analyses provide useful information, mapping their elemental concentrations along with till does not appear to be particularly helpful. A thorough understanding of the glacial events is imperative to the interpretation of geochemical results.

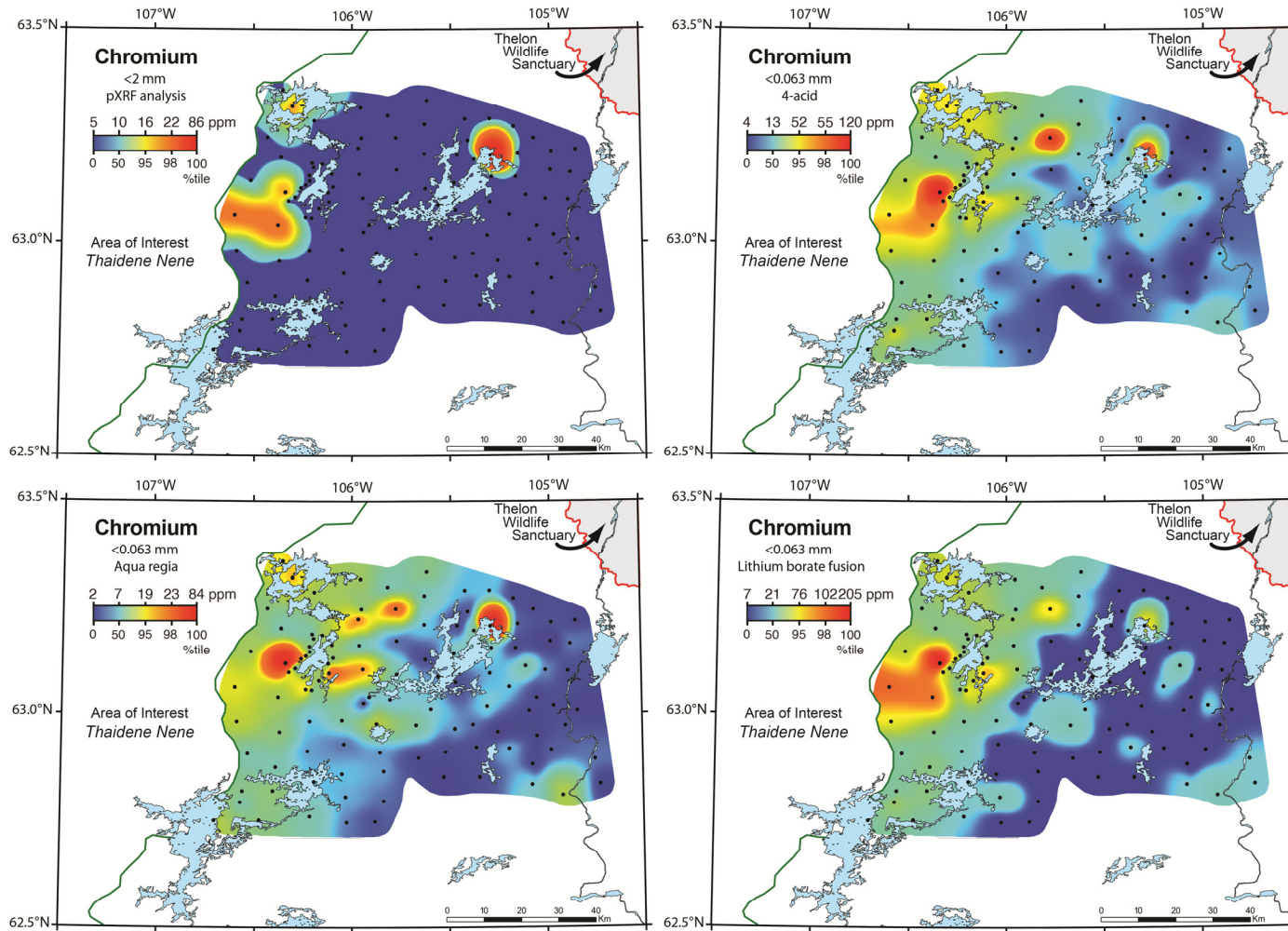


Figure 12. Chromium (Cr) in till by pXRF on the <2 mm size fraction versus ICP-MS/ES following aqua regia, 4-acid, and lithium borate fusion digestions on the <0.063 mm size fraction. Sample sites are represented by black dots.

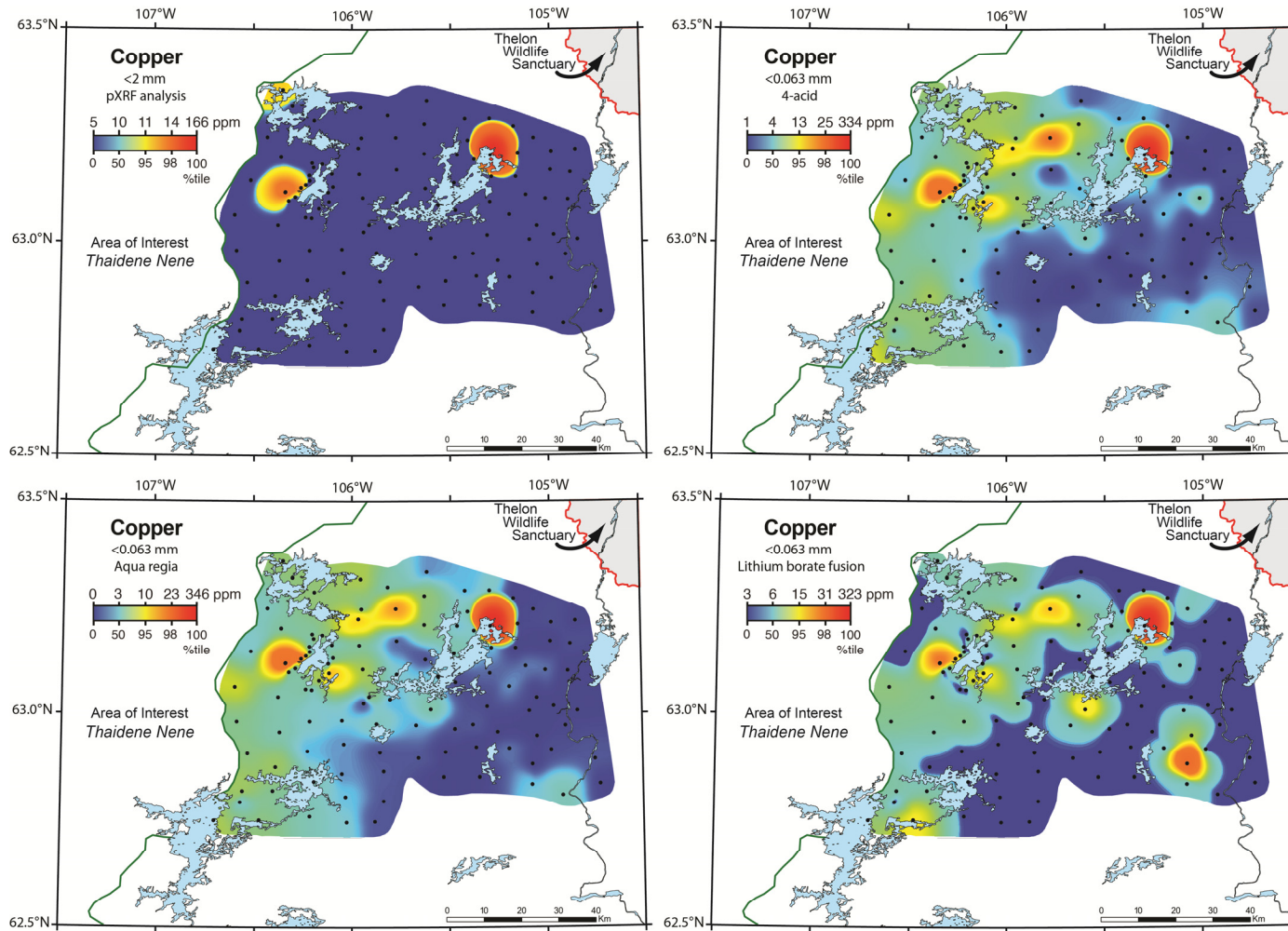


Figure 13. Copper (Cu) in till by pXRF on the <2 mm size fraction versus ICP-MS/ES following aqua regia, 4-acid, and lithium borate fusion digestions on the <0.063 mm size fraction. Sample sites are represented by black dots.

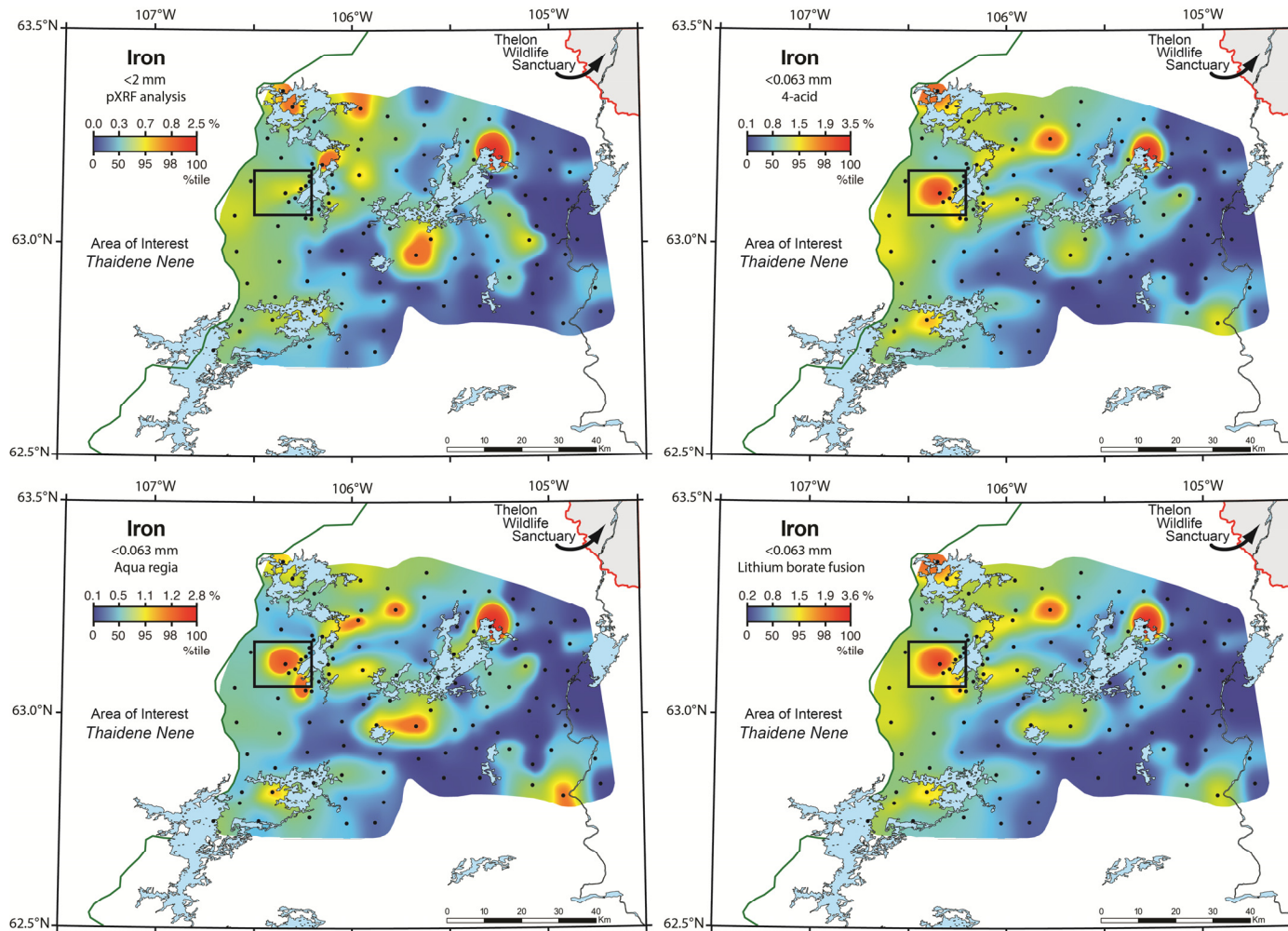


Figure 14. Iron (Fe) in till by pXRF on the <2 mm size fraction versus ICP-MS/ES following aqua regia, 4-acid, and lithium borate fusion digestions on the <0.063 mm size fraction. Sample sites are represented by black dots. Black lined box shows a region to the west of Williams Lake that is anomalous by all three laboratory methods, but not the pXRF.

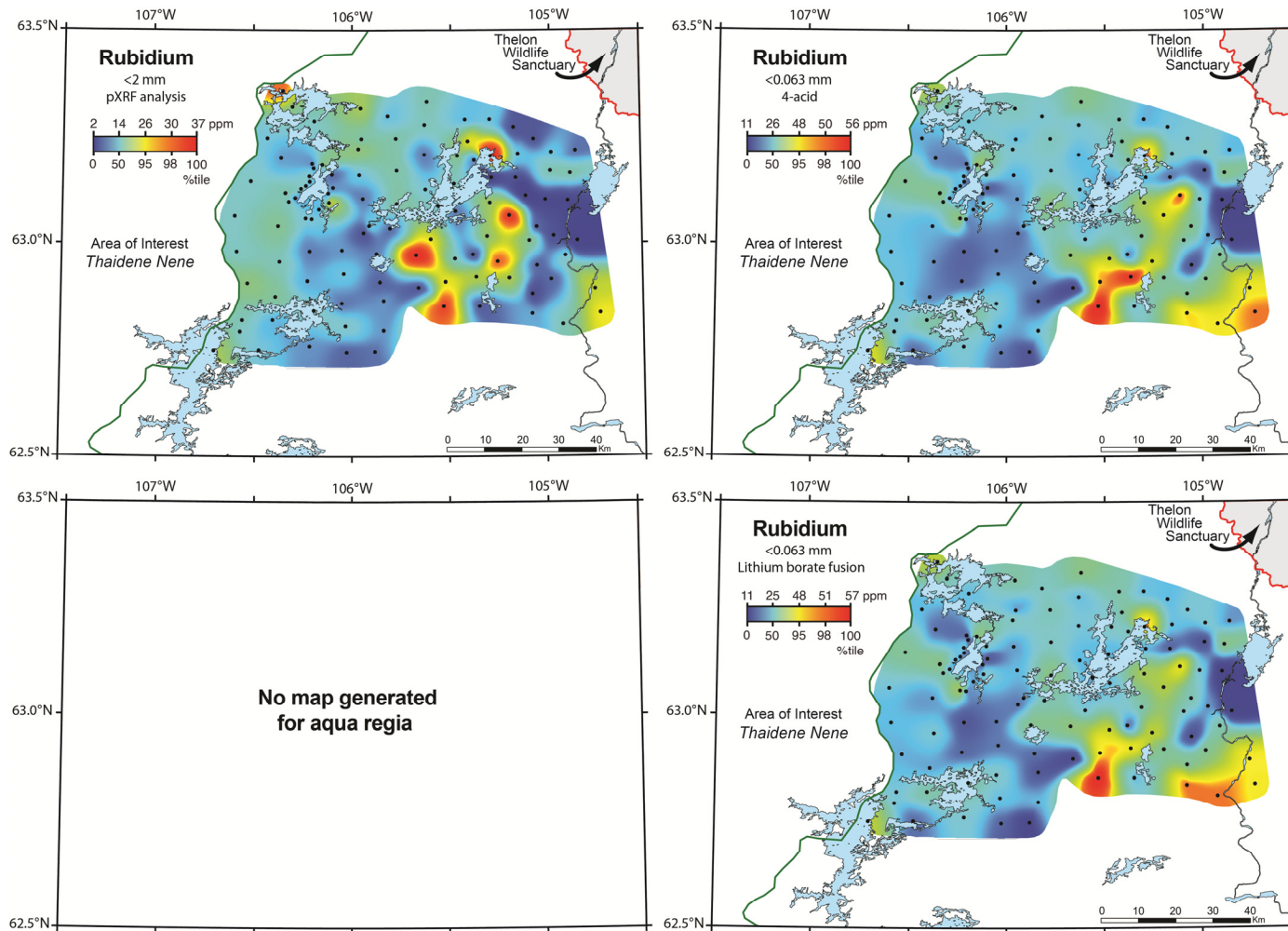


Figure 15. Rubidium (Rb) in till by pXRF on the <math><2\text{ mm}</math> size fraction versus ICP-MS/ES following aqua regia, 4-acid, and lithium borate fusion digestions on the <math><0.063\text{ mm}</math> size fraction. Sample sites are represented by black dots.

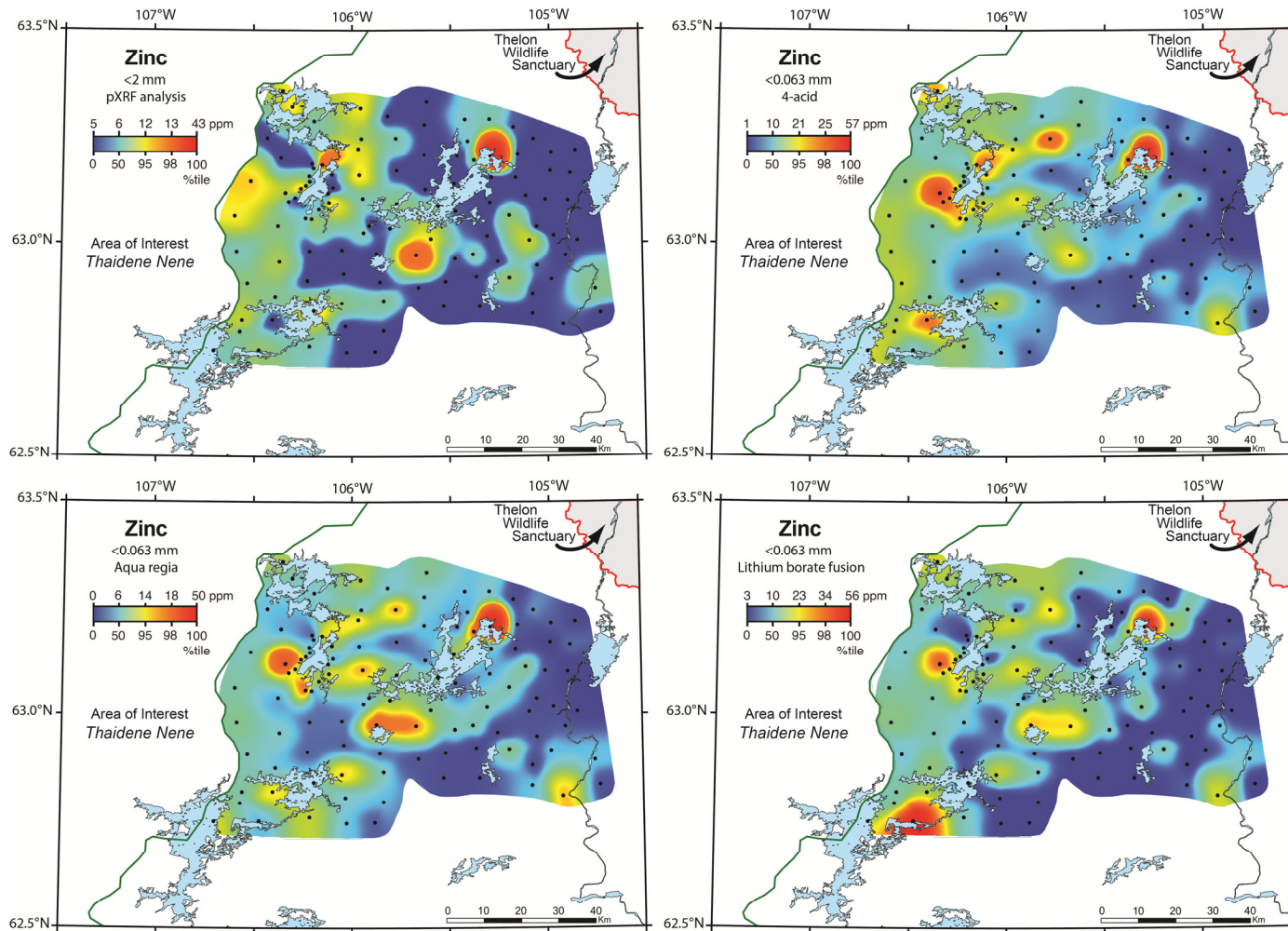


Figure 16. Zinc (Zn) in till by pXRF on the <2 mm size fraction versus ICP-MS/ES following aqua regia, 4-acid, and lithium borate fusion digestions on the <0.063 mm size fraction. Sample sites are represented by black dots.

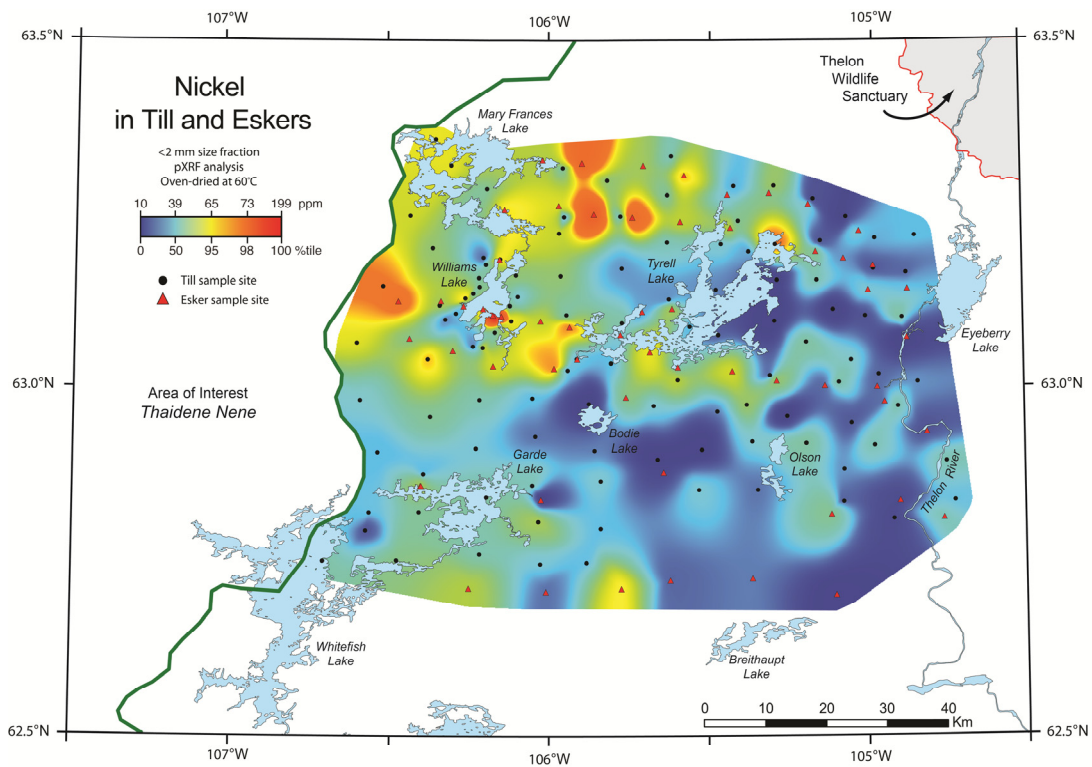
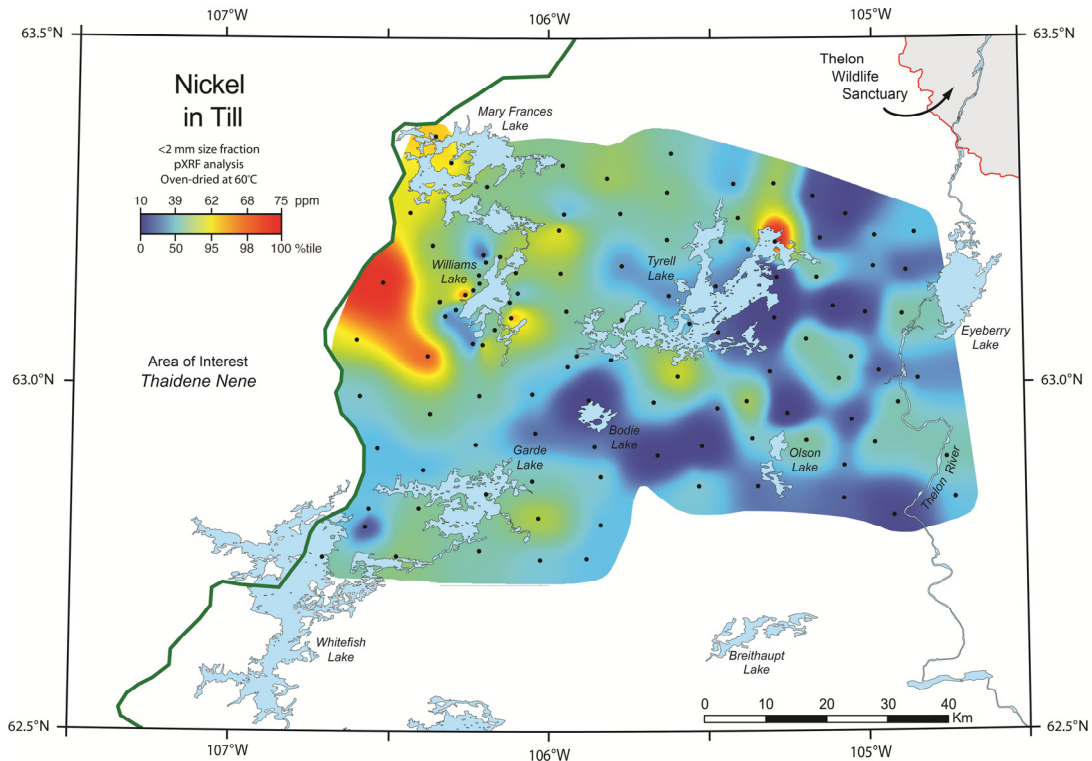


Figure 17. Nickel (Ni) by pXRF on dried and sieved (<2 mm) samples in till (top), and both till and eskers (bottom).

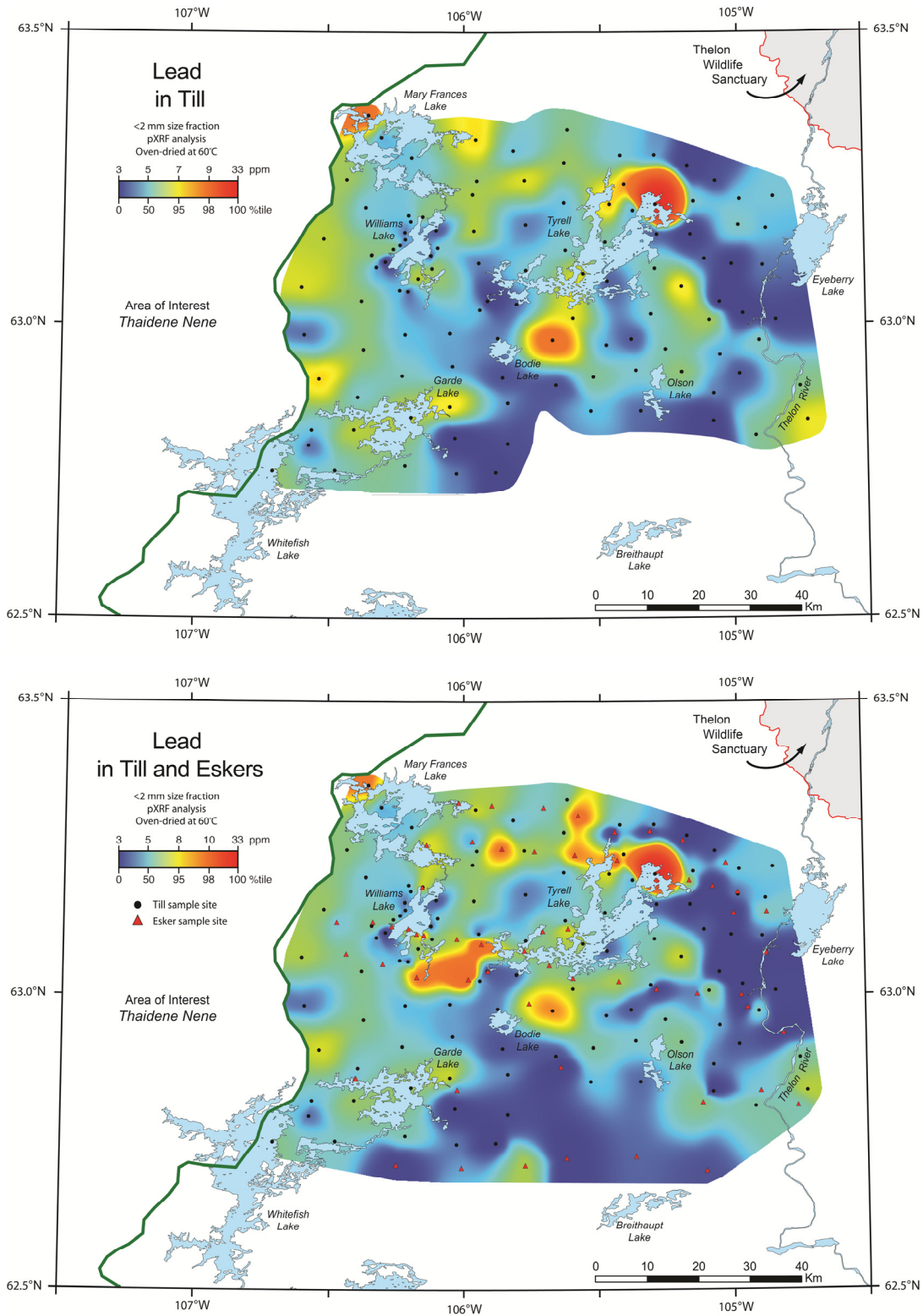


Figure 18. Lead (Pb) by pXRF on dried and sieved (<2 mm) samples in till (top), and both till and eskers (bottom).

Conclusion

Results indicate that in-field pXRF spectrometry is comparable to traditional laboratory methods and provides the additional benefits of rapid analysis and data integration into sampling designs. However, we have shown that some sample preparation (in this case drying and sieving to <2 mm) is key to obtaining high quality data.

It is advisable to dry and sieve samples to <2 mm or smaller at field camp, prior to analysis by pXRF spectrometry. A surprisingly large amount of gravel and pebbles was removed from the unprocessed sample vials, which were shown to decrease the coefficient of correlation with the prepared <2mm. For many projects, pXRF spectrometry makes analyzing esker samples worthwhile given its time- and cost-effectiveness. However since differences between till and esker were seen to make true regional trends and anomalies in till less apparent, we recommend mapping or plotting the two data sets separately.

Interpolated maps produced with data acquired from pXRF spectrometry successfully illustrate the regional geochemical trends, and most importantly, the significant geochemical anomalies in the surficial samples. These pXRF derived maps are comparable to geochemical maps produced using traditional laboratory analytical methods, demonstrating that with minimal sample preparation pXRF spectrometry can quickly provide regional geochemical trends, and identify anomalous areas. This information can make field projects more cost-effective, if it is used to identify regions of interest, and prioritize samples to be analyzed using traditional geochemical methods. Portable XRF spectrometry also allows for better in-field time management, as a tool to prioritize resources to re-sample specific sub-regions at higher density and/or map in more detail the regions of interest.

We conclude that pXRF spectrometry is a viable tool for analyzing surficial sediments and, given its time- and cost-effectiveness, a wide variety of field projects could benefit from this method.

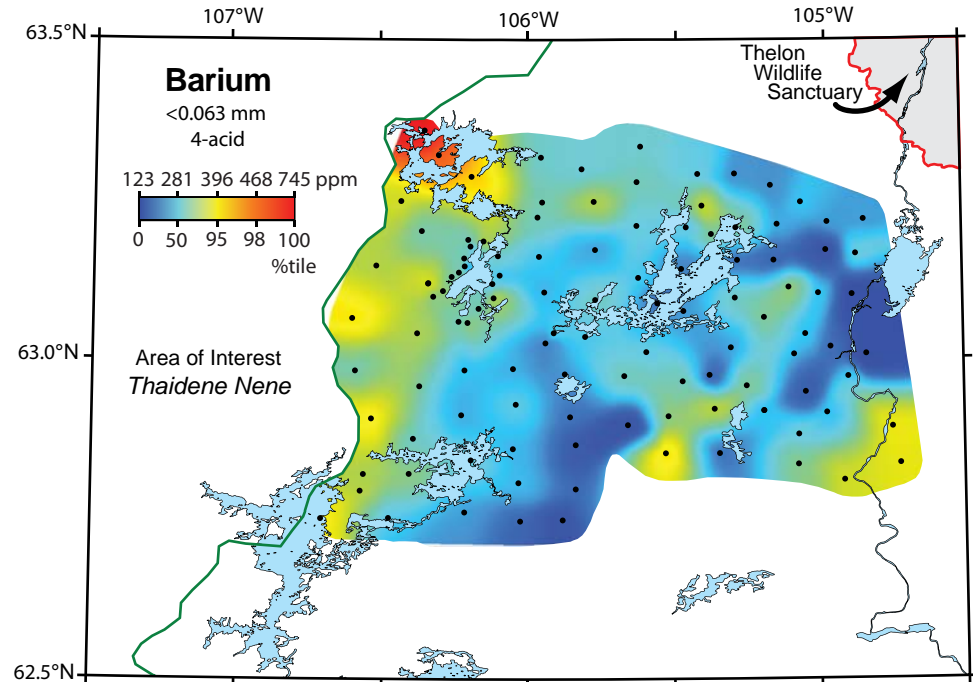
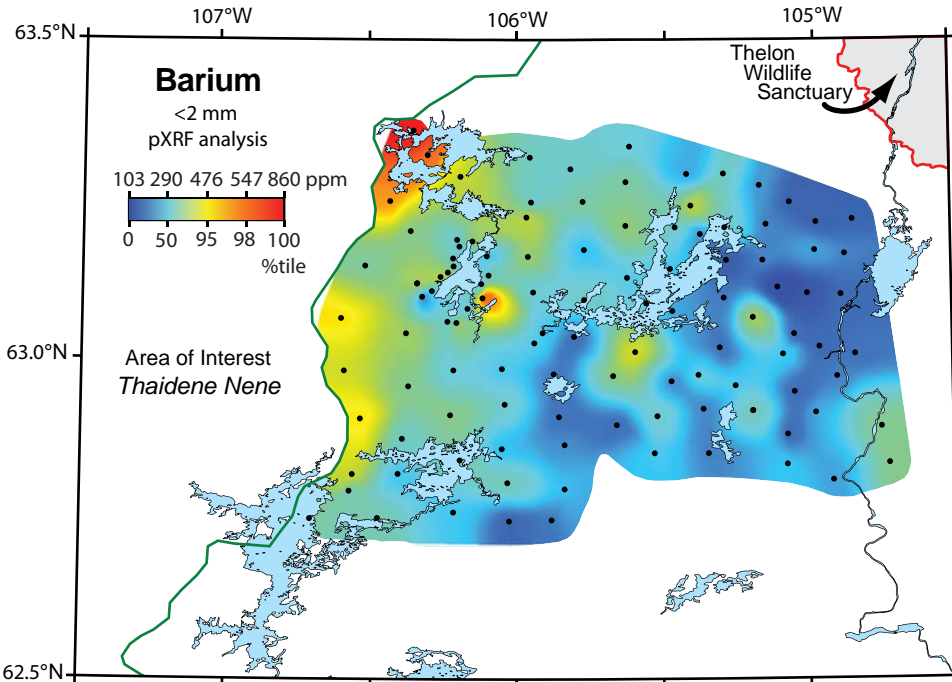
References

- Aylsworth, J.M. and Shilts, W.W., 1989a. Glacial features around the Keewatin Ice Divide: Districts of Mackenzie and Keewatin. Geological Survey of Canada, Paper, 88-24, 21p.
- Aylsworth, J.M and Shilts W.W., 1989b. Glacial features around the Keewatin Ice Divide: Districts of Mackenzie and Keewatin, Geological Survey of Canada, Map 24-1987, scale 1:1 000 000.
- Craig, B.G., 1964. Surficial geology of east-central District of Mackenzie, Northwest Territories. Geological Survey of Canada, Bulletin 99.

- Kjarsgaard, B.A., Knight, R.D., Plourde, A.P., Sharpe, D.R., and Lesemann, J-E., 2013a. Geochemistry of till samples, NTS 75-I, 75-J, 75-O, 75-P (Mary Frances Lake — Whitefish Lake — Thelon River area), Northwest Territories. Geological Survey of Canada, Open File 7351, 26 p.
- Kjarsgaard, B.A., Knight, R., Sharpe, D. R., Kerr, D., Cummings, D.I. and Russell, H.A.J., and Lemkow, D., 2013b. Significance of indicator minerals from till and esker samples, Thaidene Nene MERA study area, *in* Wright, D.F., Ambrose, E.J., Lemkow, D., and Bohnam-Carter, G.F. (ed.), 2013. Mineral and energy resource assessment of the proposed Thaidene Nene National Park Reserve in the area of the East Arm of Great Slave Lake, Northwest Territories; Geological Survey of Canada, Open File 7196. doi:10.4095/292447
- Knight, R.D., Moroz, M., and Russell, H.A.J., 2012. Geochemistry of a Champlain Sea aquitard: portable XRF analysis. Geological Survey of Canada, Open File 7085, 35 p.
- Knight, R.D., Kjarsgaard, B.A., Plourde, A.P., and Moroz, M., 2013. Portable XRF spectrometry of standard reference materials with respect to precision, accuracy, dwell time optimization, instrument drift, and calibration. Geological Survey of Canada, Open File 7358, 42p.
- Lee, H.A., Craig, B.G. and Fyles, J.G., 1957. Keewatin Ice Divide. Geological Society of America Bulletin, 68, p. 1760-1761.
- Lee, H. A., 1959. Surficial geology of southern District of Keewatin, and the Keewatin Ice Divide, Northwest Territories. Geological Survey of Canada, Bulletin 51, 42 p.
- Lynch, J., 1996. Provisional elemental values for four new geochemical soil and till reference materials, TILL-1, TILL-2, TILL-3 and TILL-4. Geostandards Newsletter, v. 20, n. 2, p. 277-287.
- NORMIN.DB, 2011. The northern minerals database. Northwest Territories Geoscience office, Yellowknife, NWT. <http://www.nwtgeoscience.ca/normin/>. Web site accessed June 2013.
- Pehrsson, S.J., Currie, M., Paul, D., Ashton, K., Harper, C., Jefferson, C., Berman, R., Martel, E., Card, C., and Peterson, T.D., 2013. Bedrock geology of southern Rae and southwestern Hearne provinces; Geological Survey of Canada, Open File 5744, scale 1:550 000, in press.
- Prest, V.K., Grant, D.R. and Rampton, V.N., 1968. Glacial Map of Canada, Geological Survey of Canada, Map 1253A: scale 1:5 000 000.
- Plourde, A.P., Knight, R.D., and Russell, H.A.J., 2012. Portable XRF spectrometry of in-situ and processed glacial sediment from a borehole within the Spiritwood buried valley, southwest Manitoba. Geological Survey of Canada, Open File 7262, 30 p.

Shaw, J., Sharpe, D. R., and Harris, J., 2010. A flowline map of glaciated Canada based on remote sensing data. *Canadian Journal of Earth Sciences*, 47, p. 89–101.

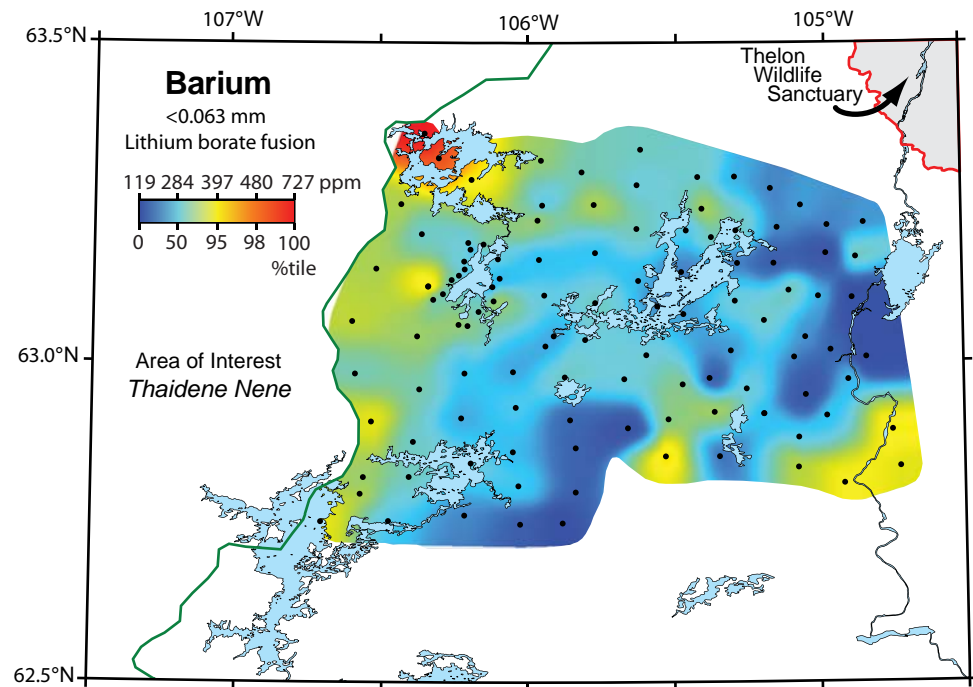
Wright, D.F., Ambrose, E.J., Lemkow, D., and Bohnam-Carter, G.F. (ed.), 2013. Mineral and energy resource assessment of the proposed Thaidene Nene National Park Reserve in the area of the East Arm of Great Slave Lake, Northwest Territories; Geological Survey of Canada, Open File 7196. doi:10.4095/292447

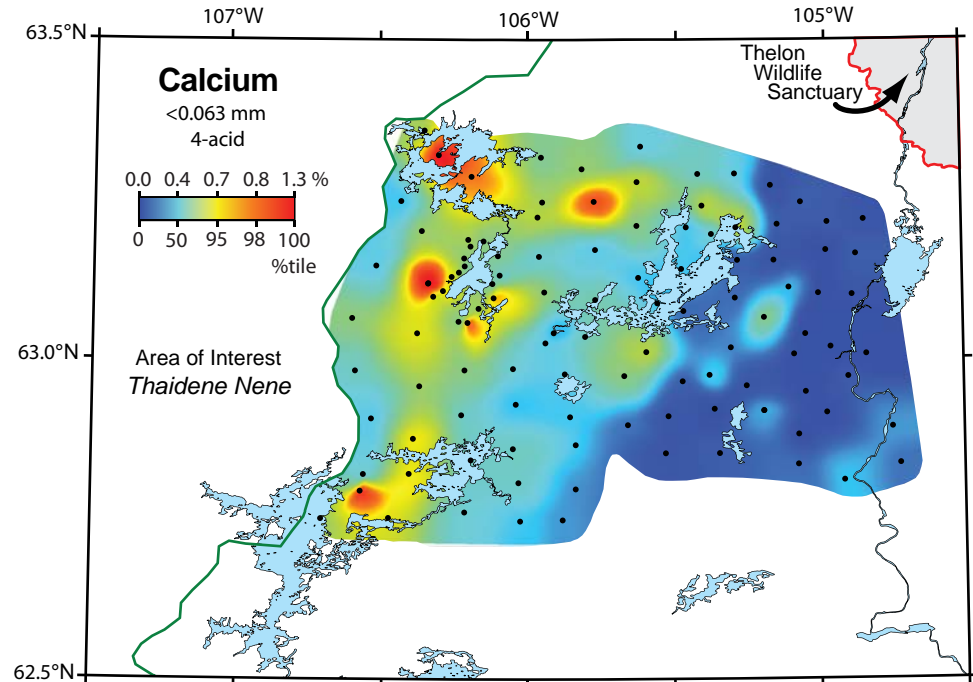
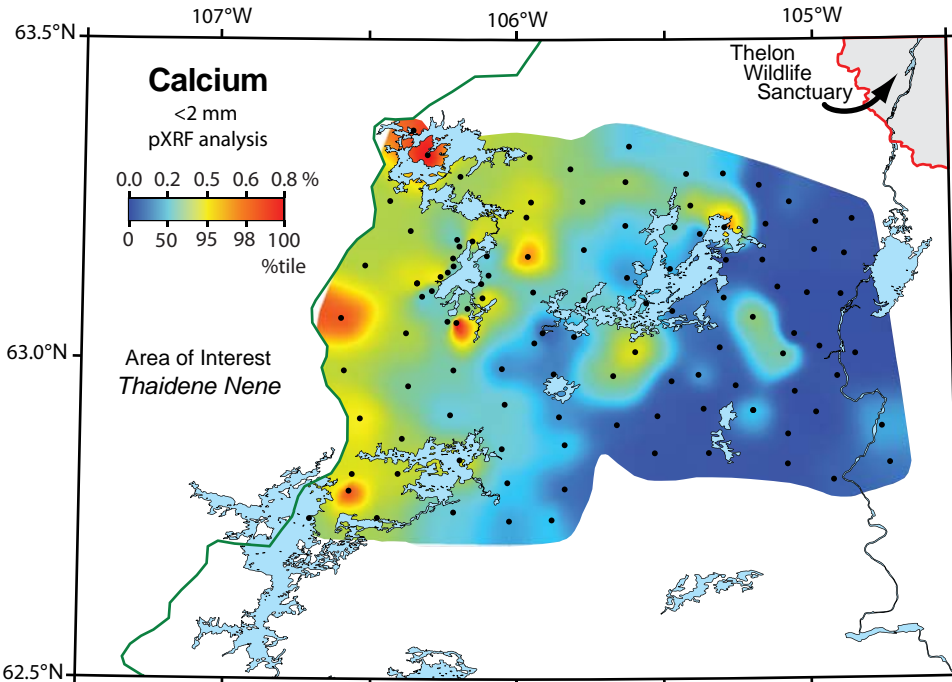


63.5°N 107°W 106°W 105°W
63.0°N
62.5°N

**No map generated
for aqua regia**

This panel indicates that no map was generated for the aqua regia digestion method. The geographic coordinates and the 'Area of Interest Thaidene Nene' boundary are consistent with the other maps in the figure.

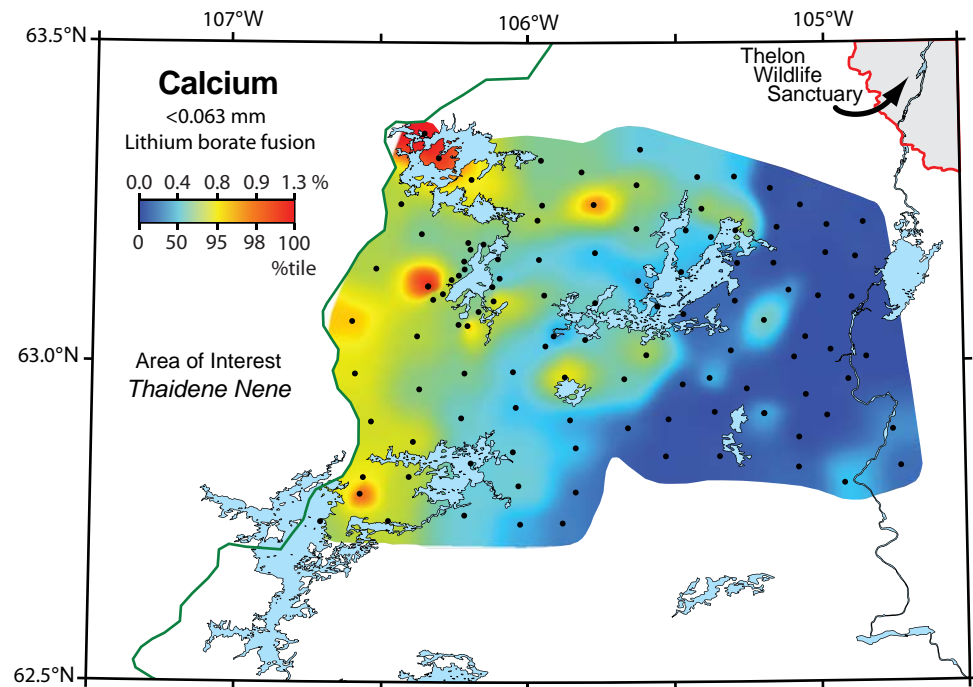


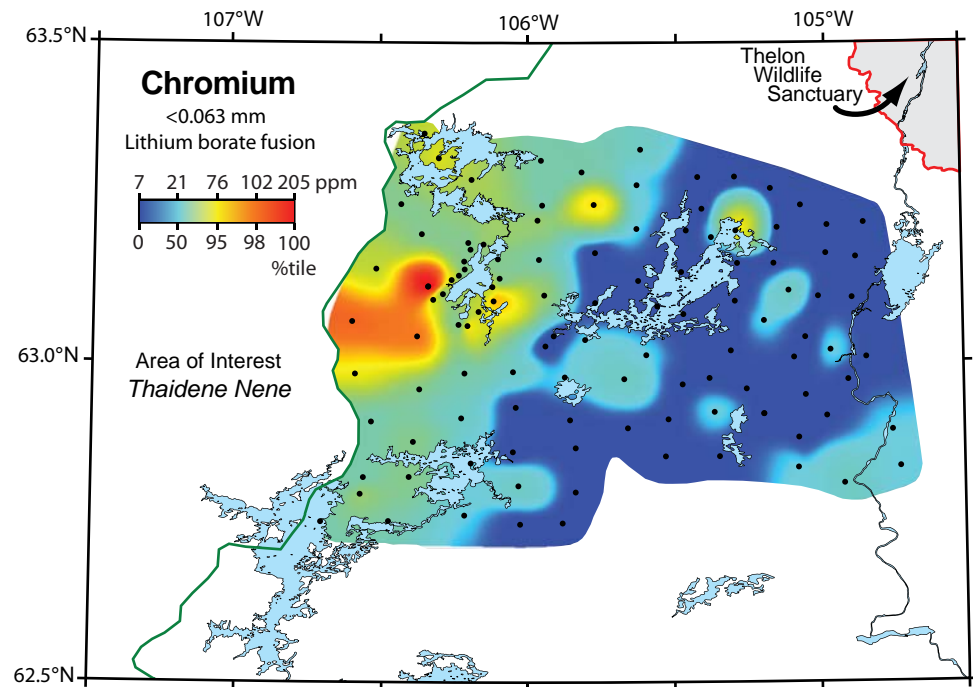
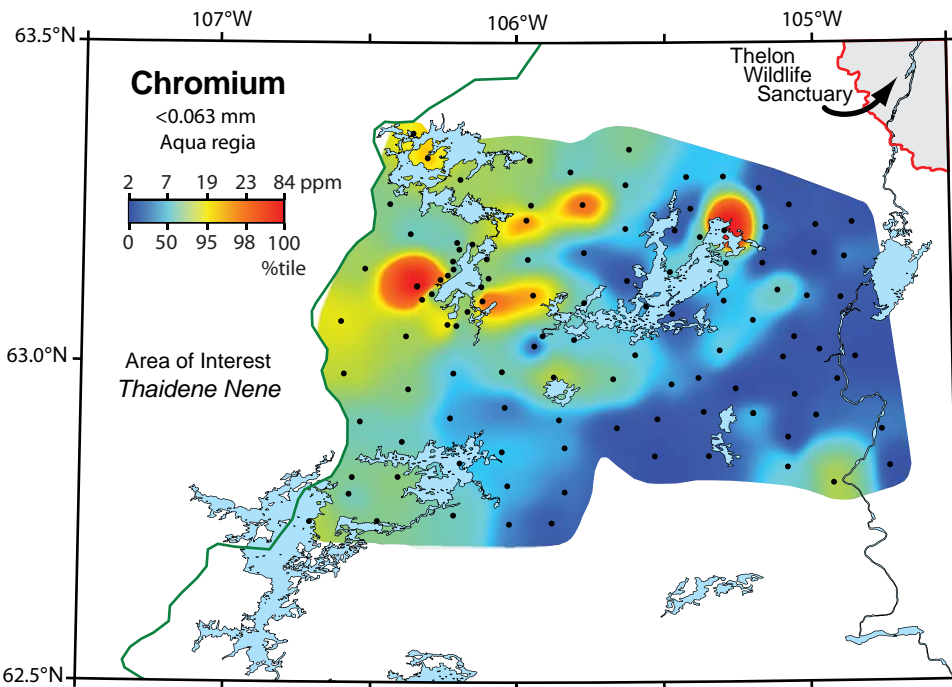
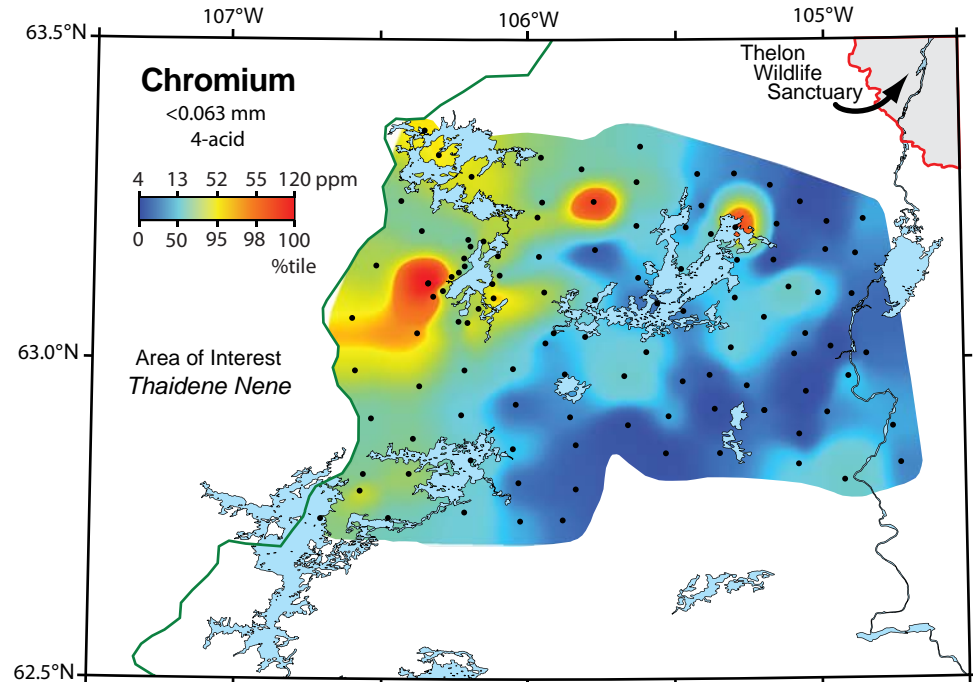
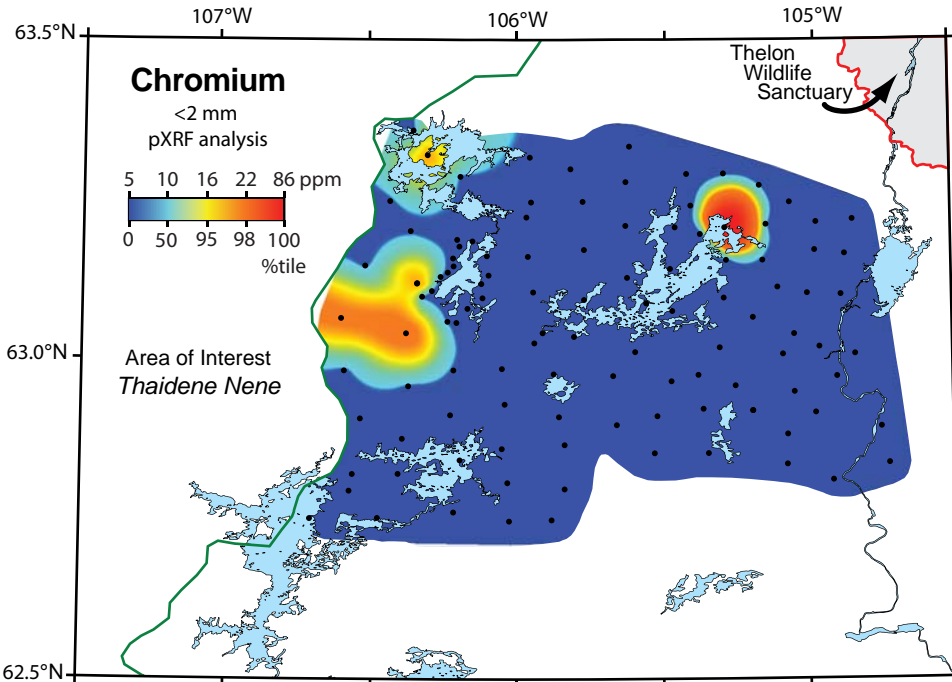


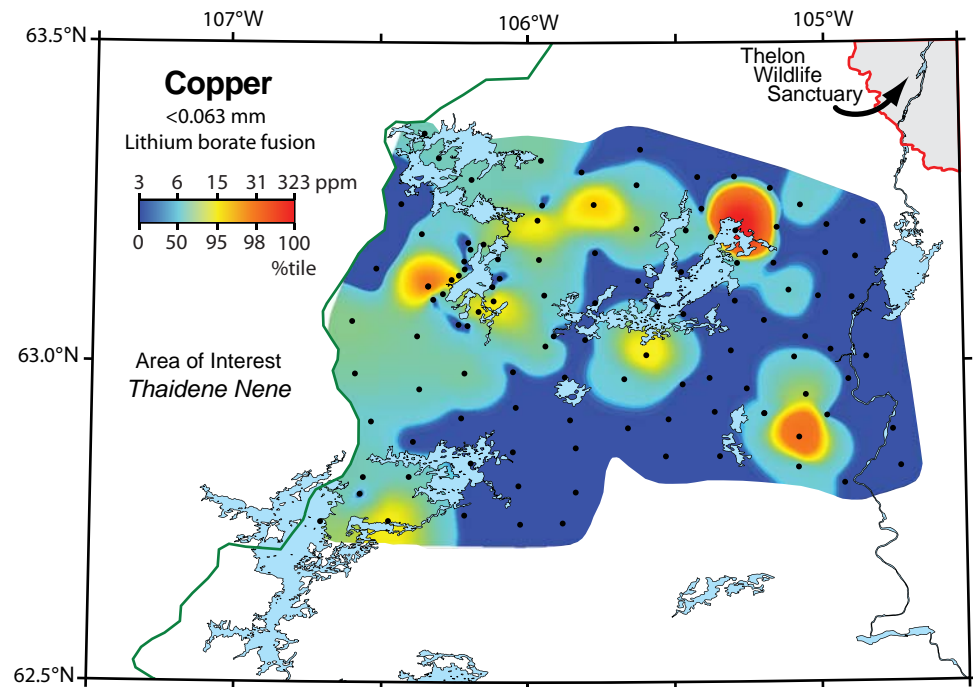
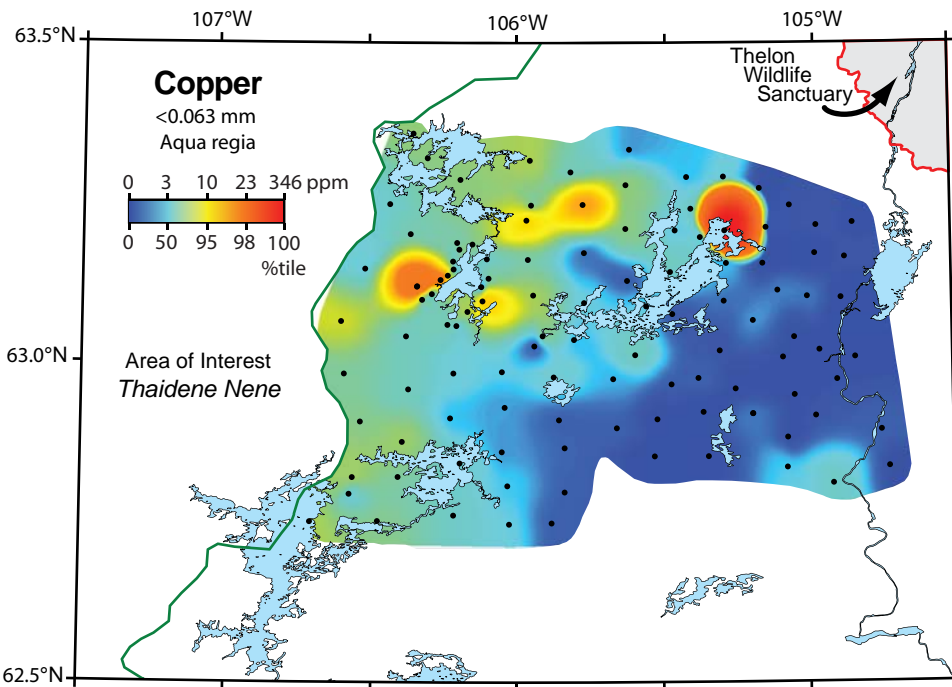
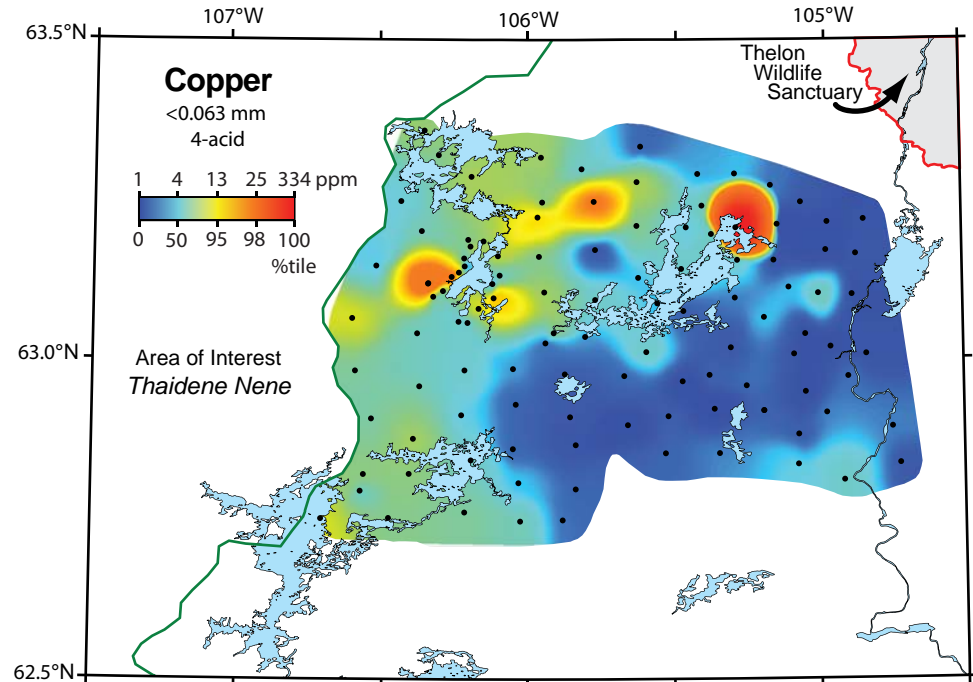
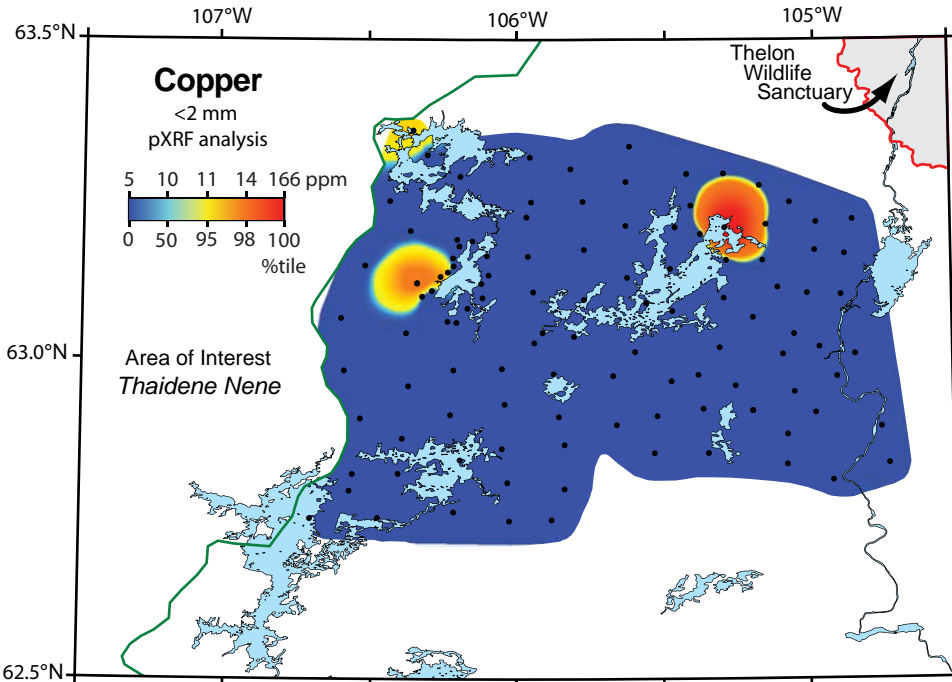
63.5°N 107°W 106°W 105°W
63.0°N
62.5°N

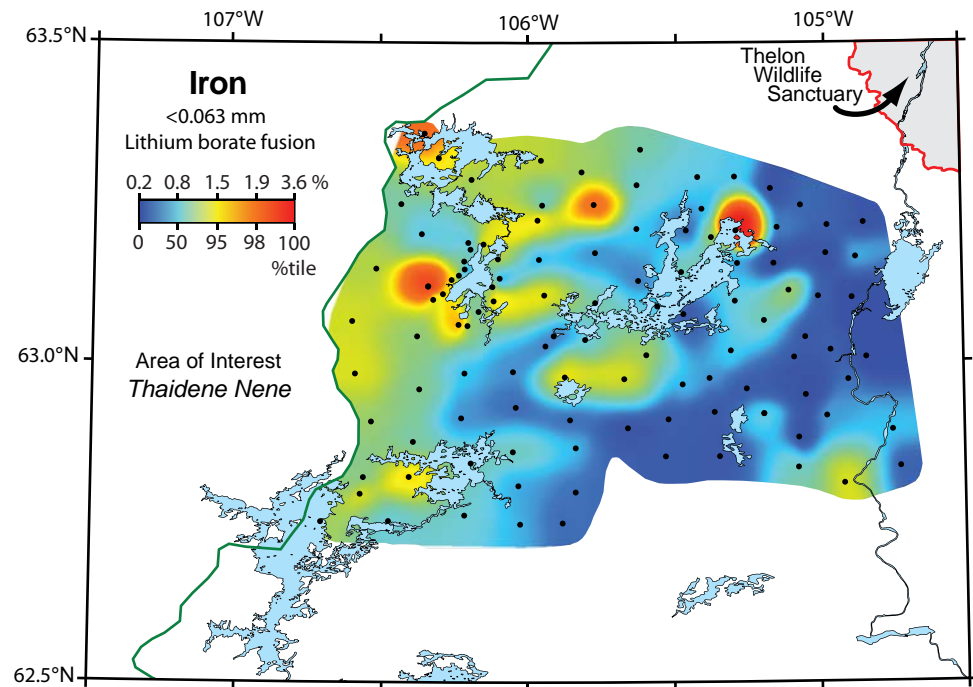
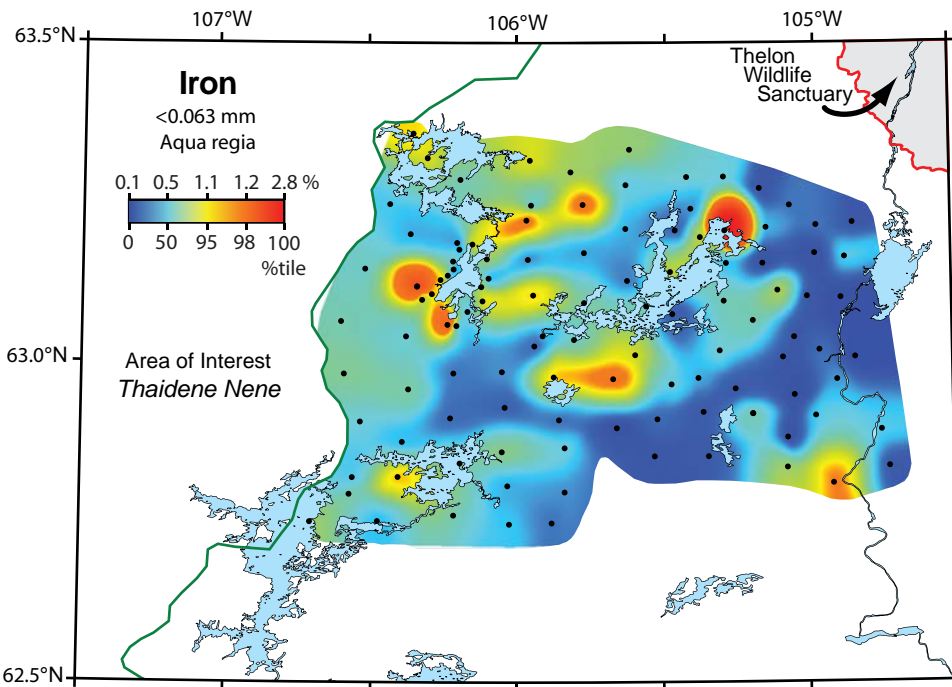
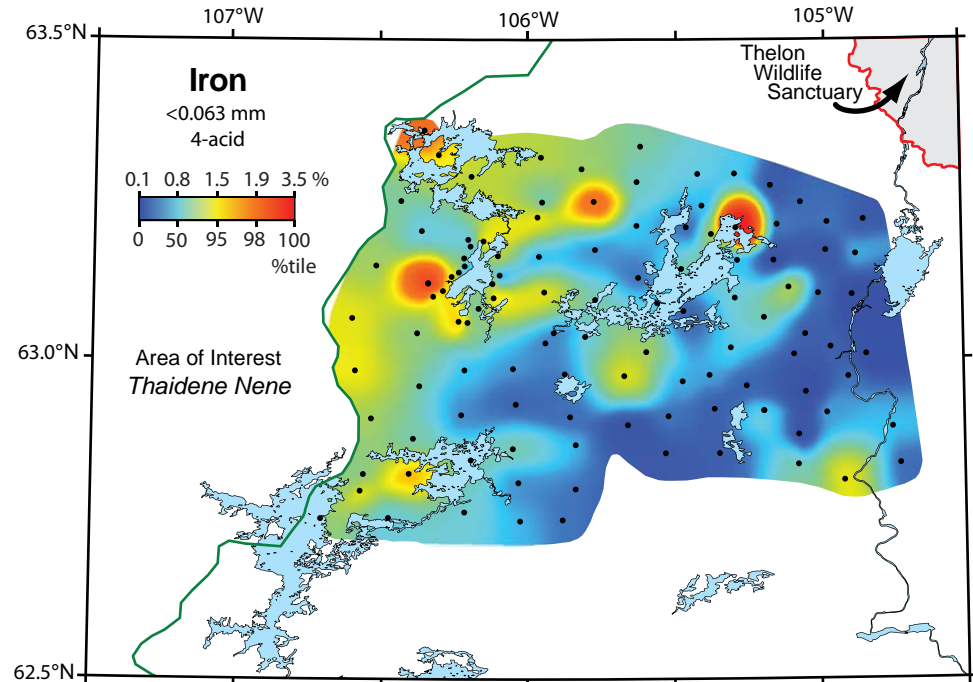
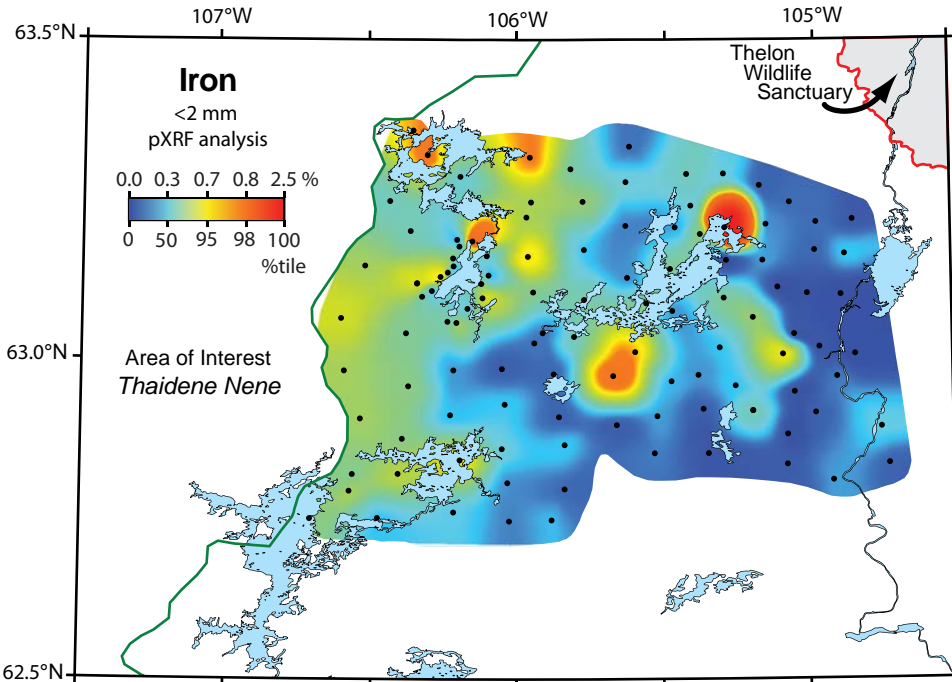
**No map generated
for aqua regia**

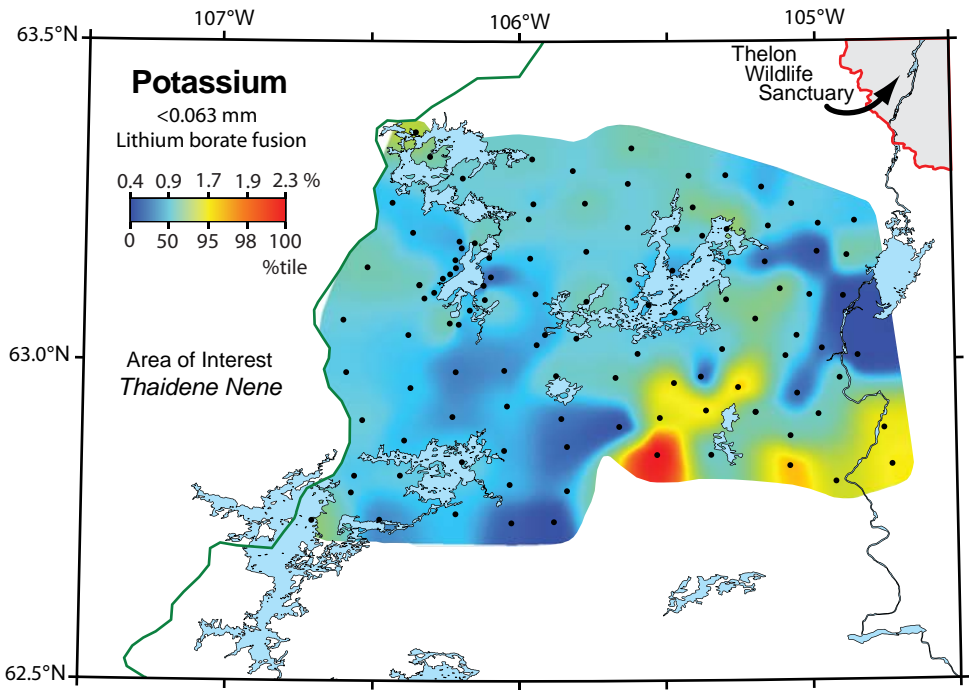
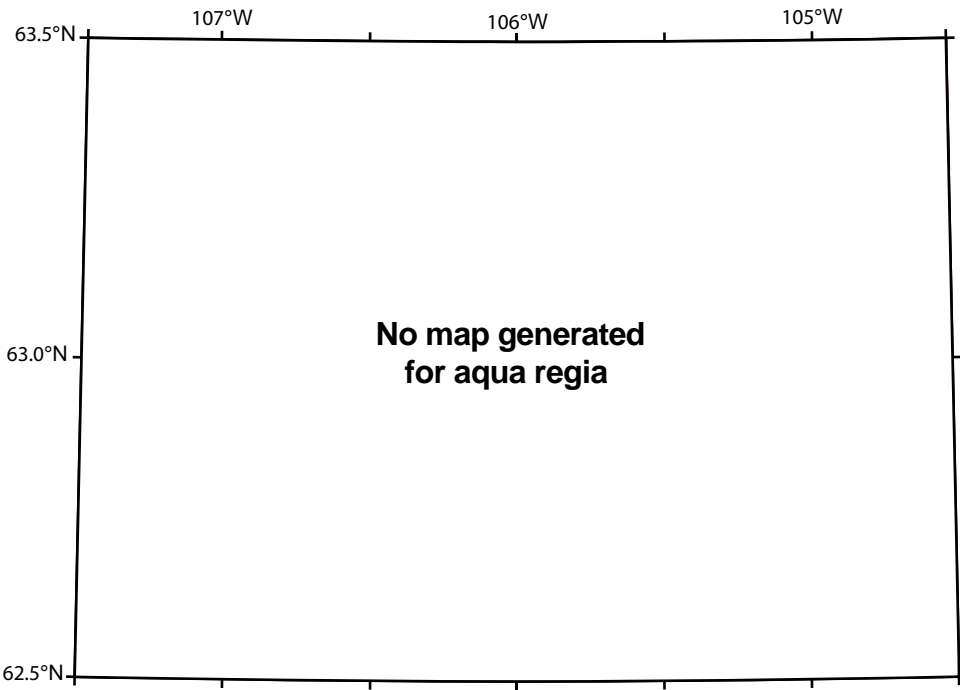
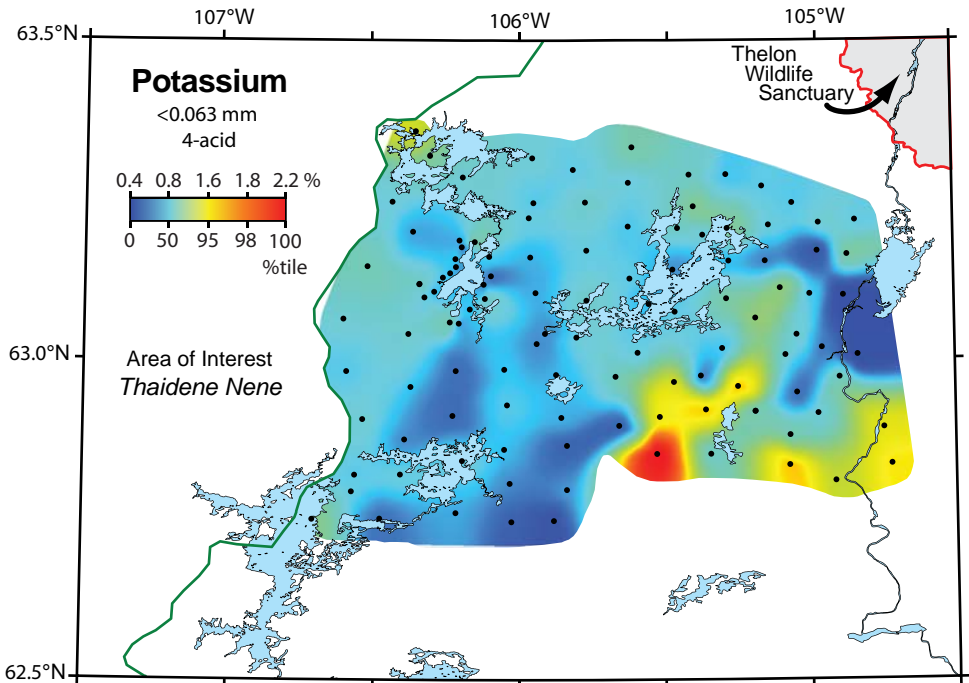
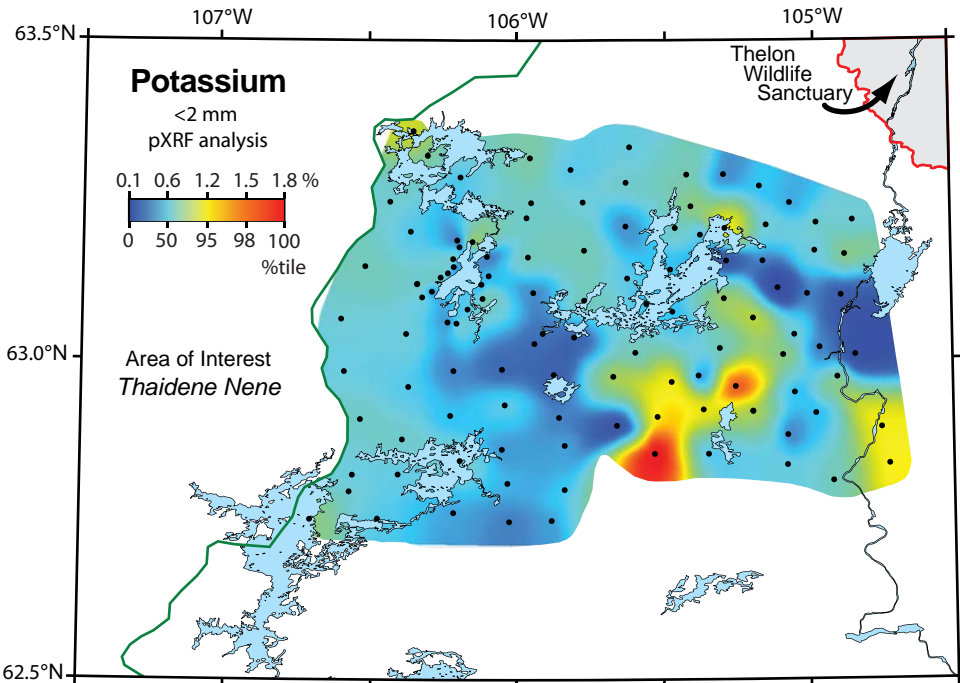
This panel is a placeholder for a map that was not generated. It contains the same geographic grid and labels as the other maps in the figure, but the central area is empty except for the text "No map generated for aqua regia".

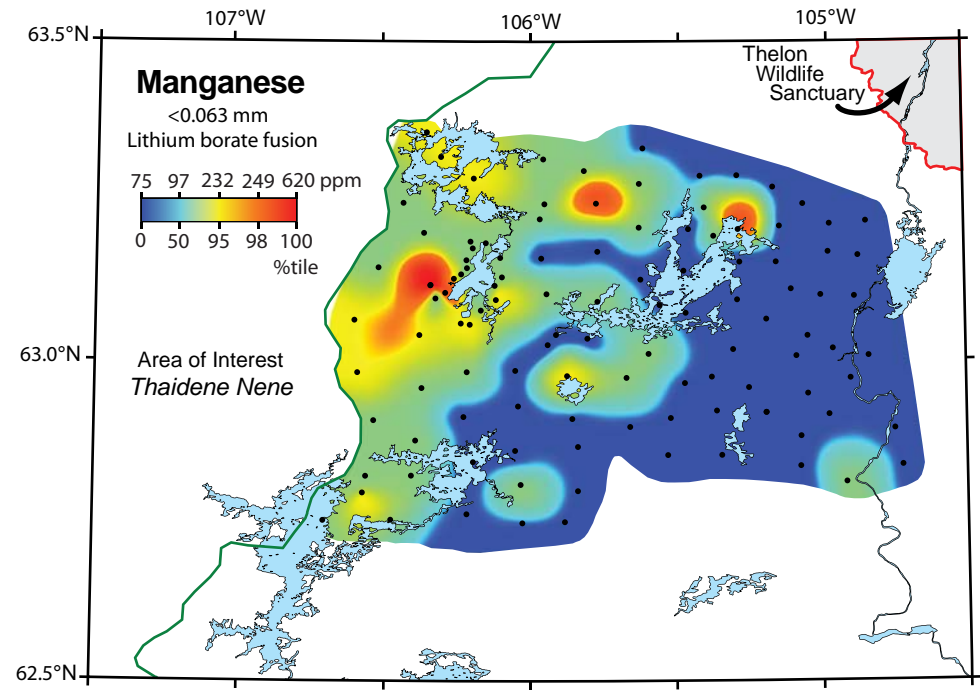
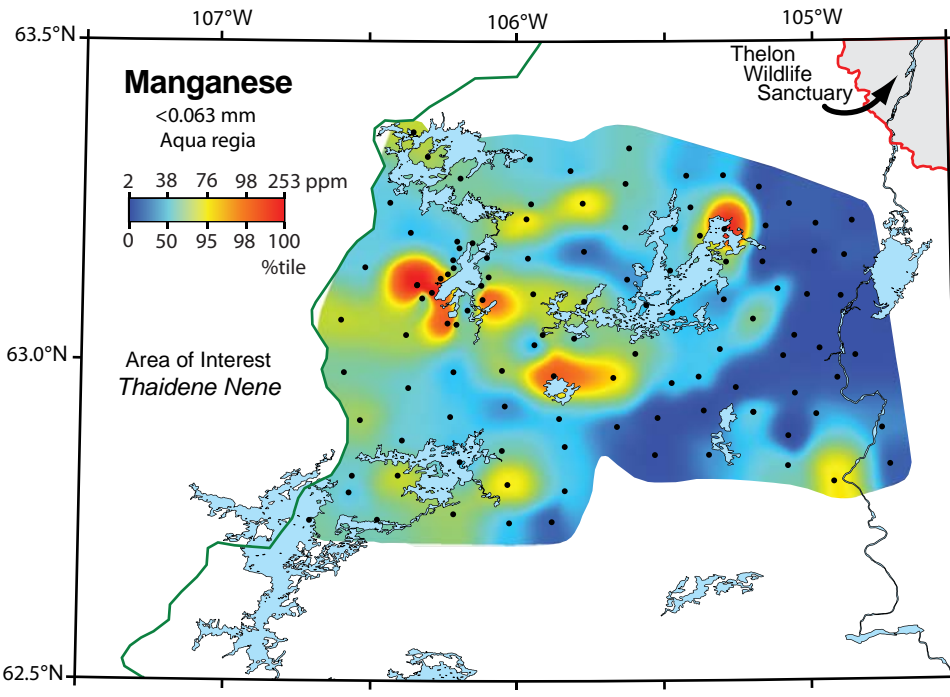
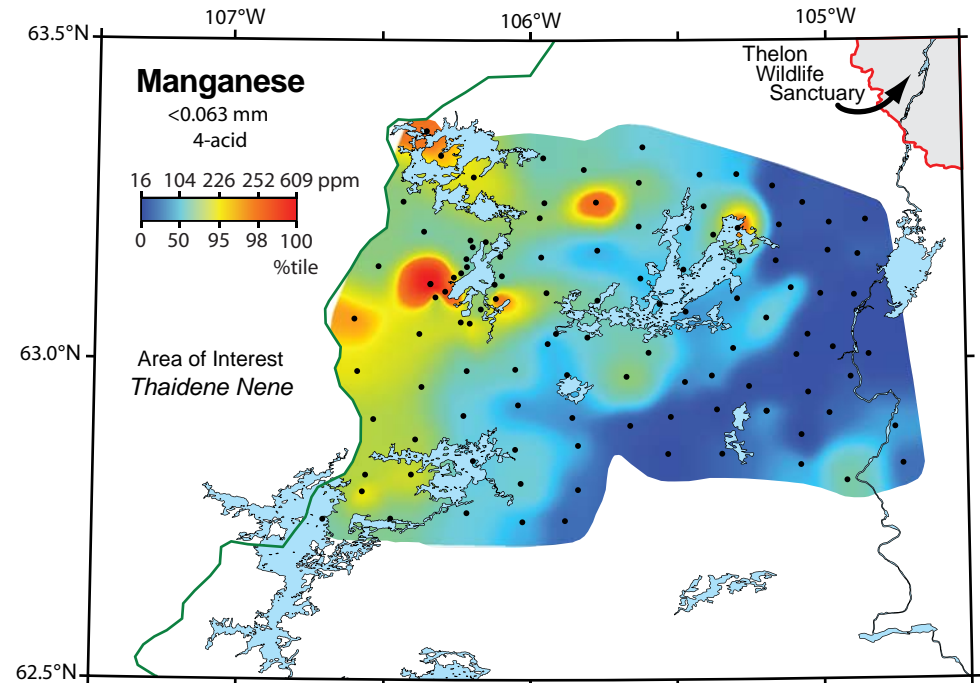
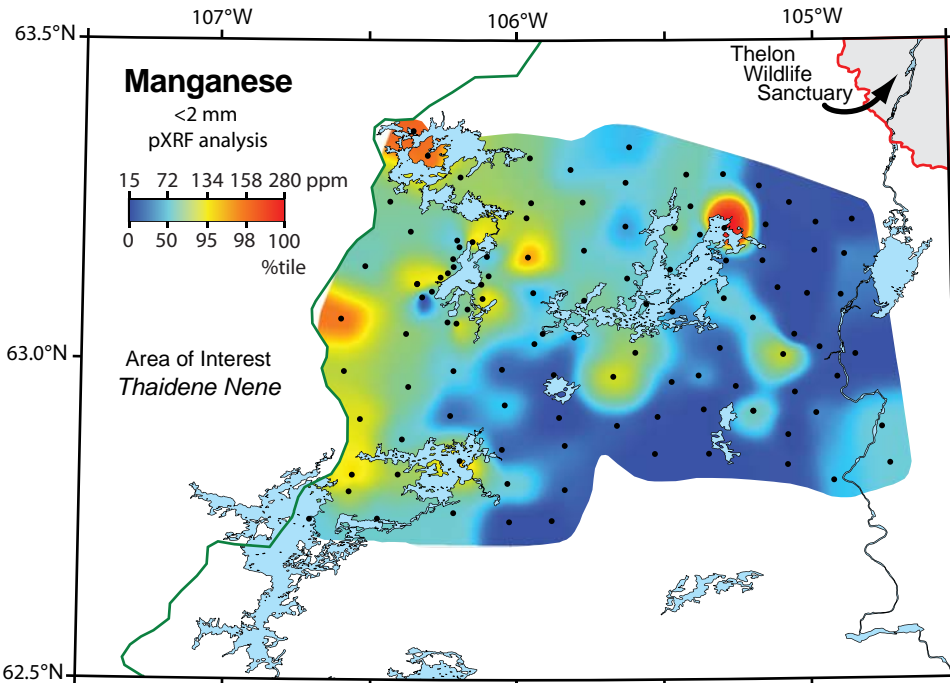


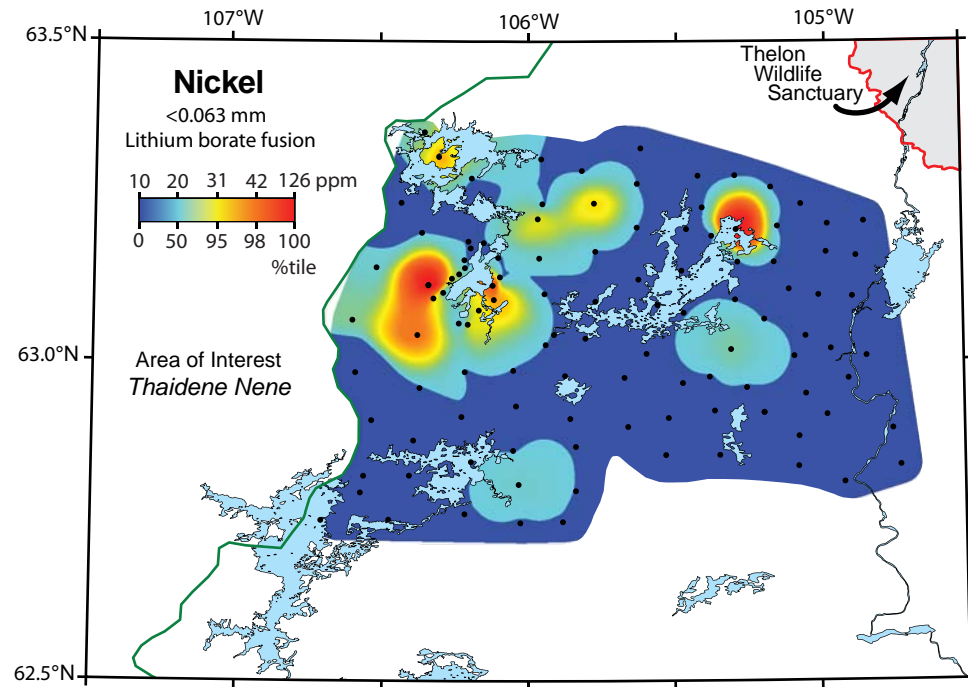
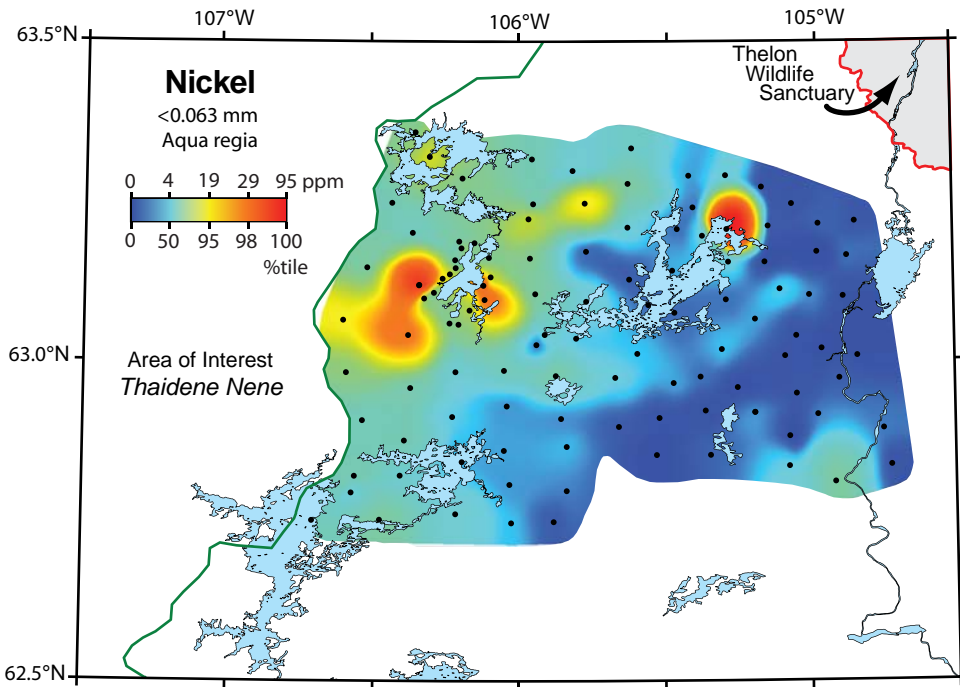
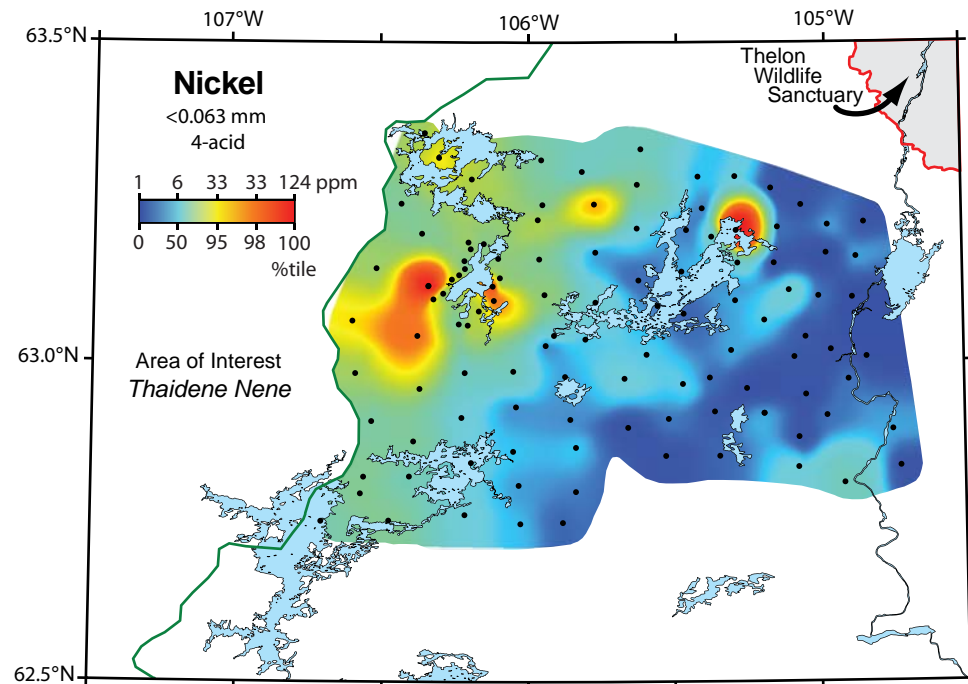
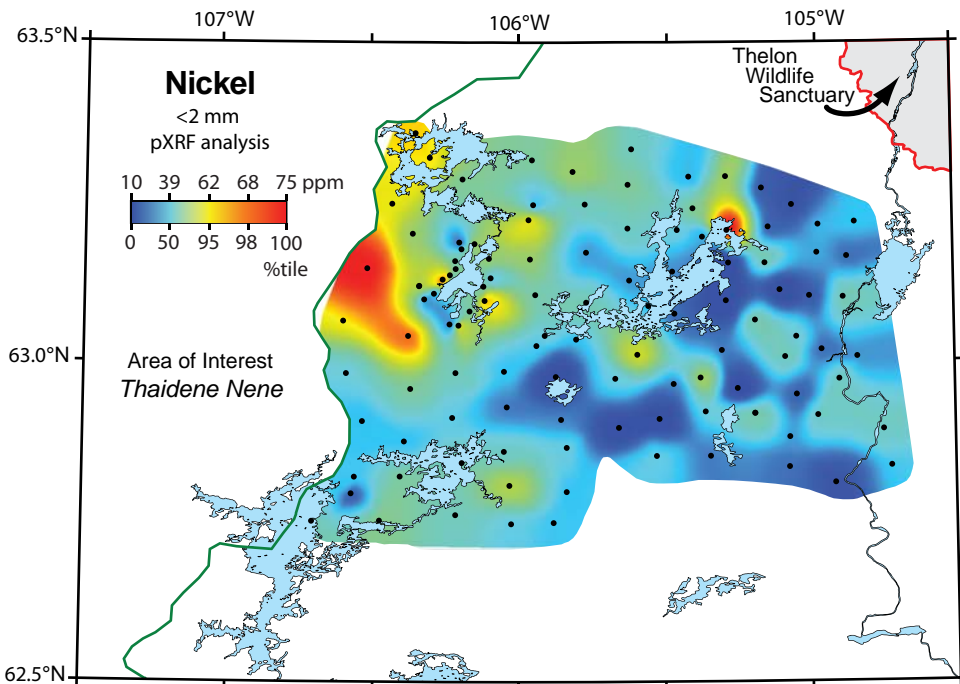


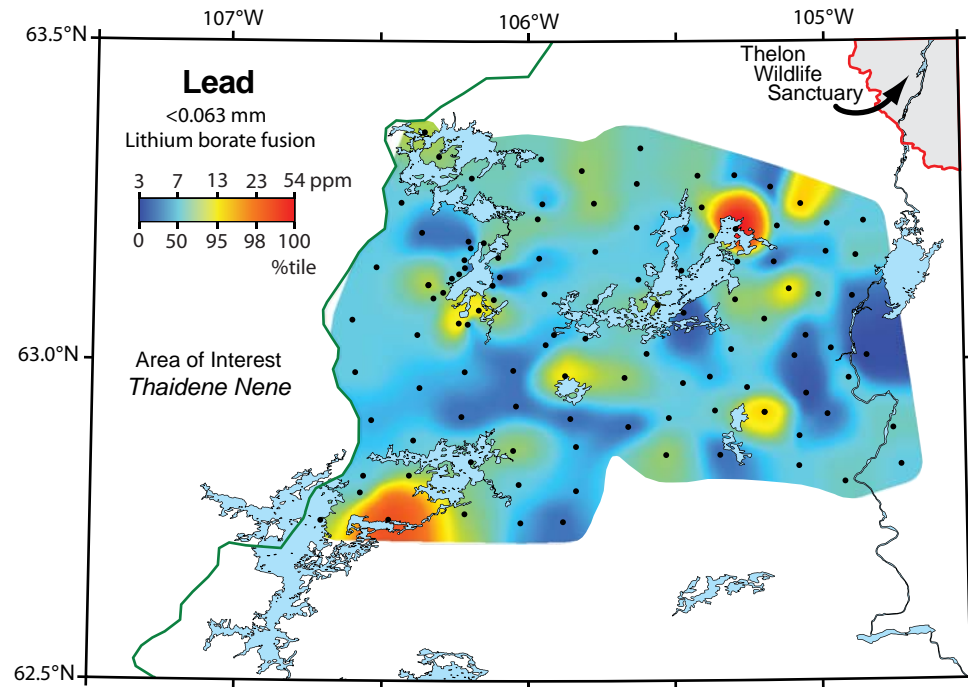
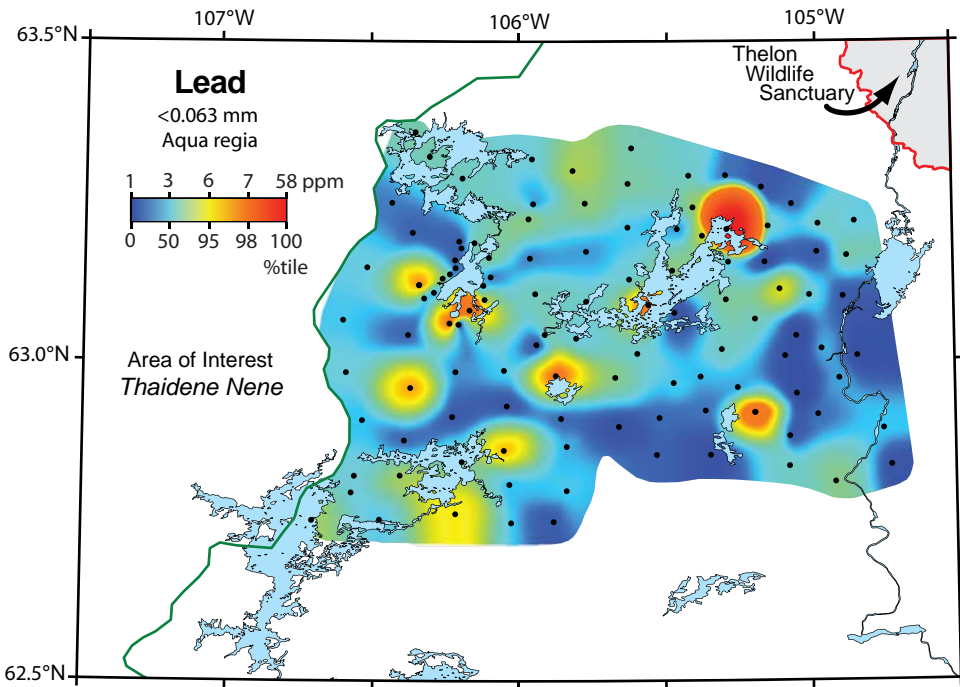
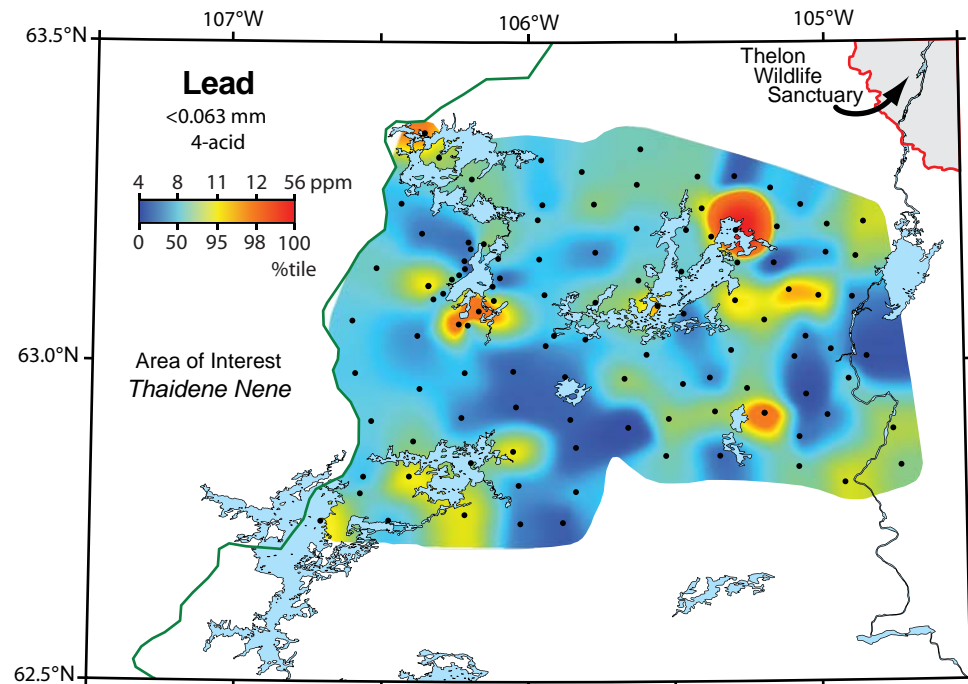
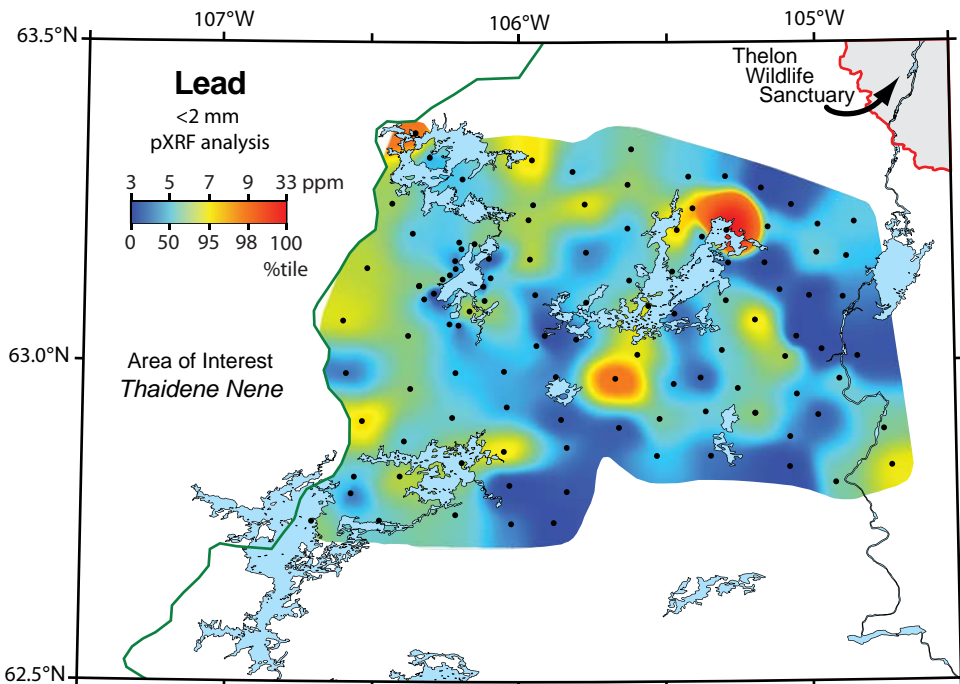


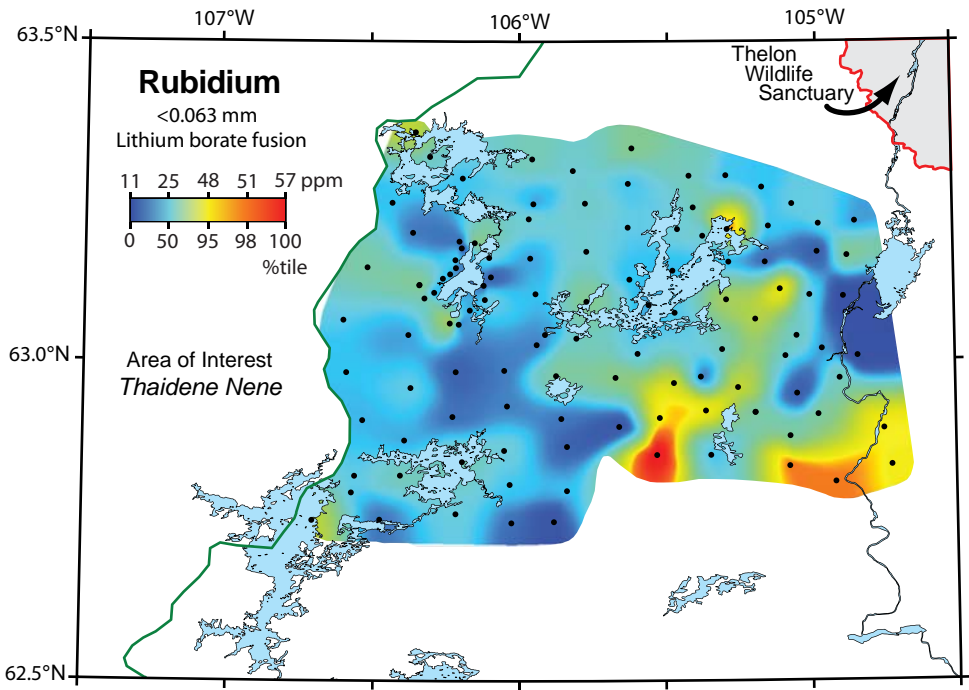
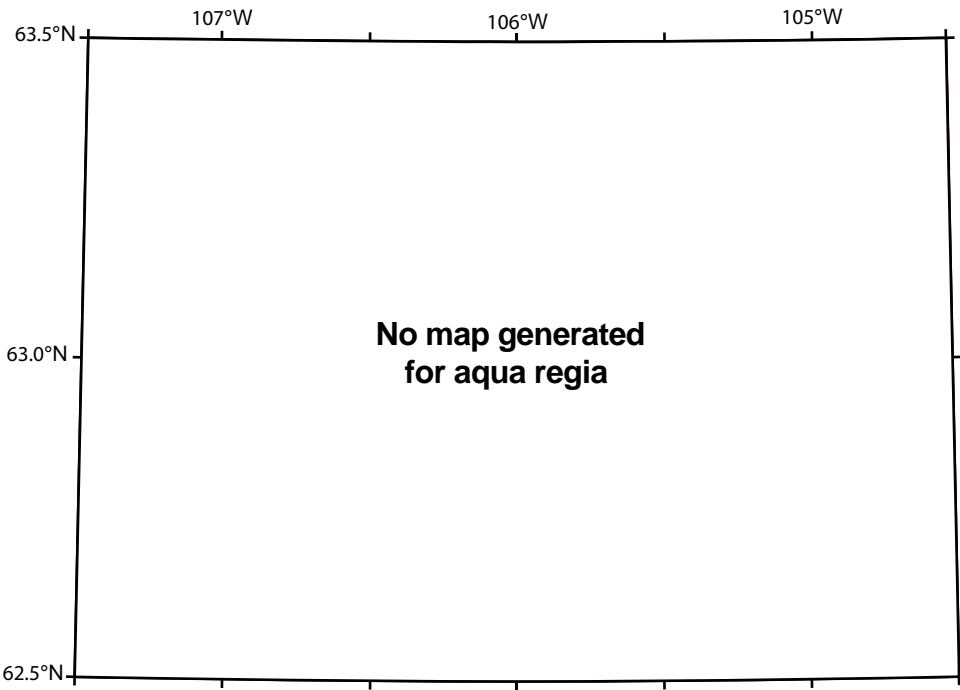
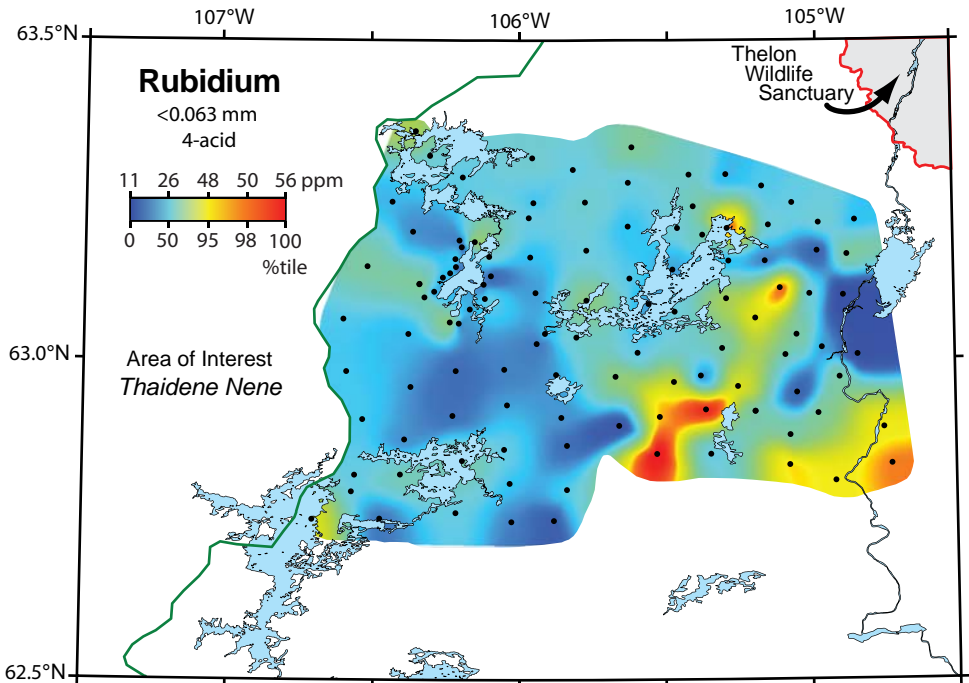
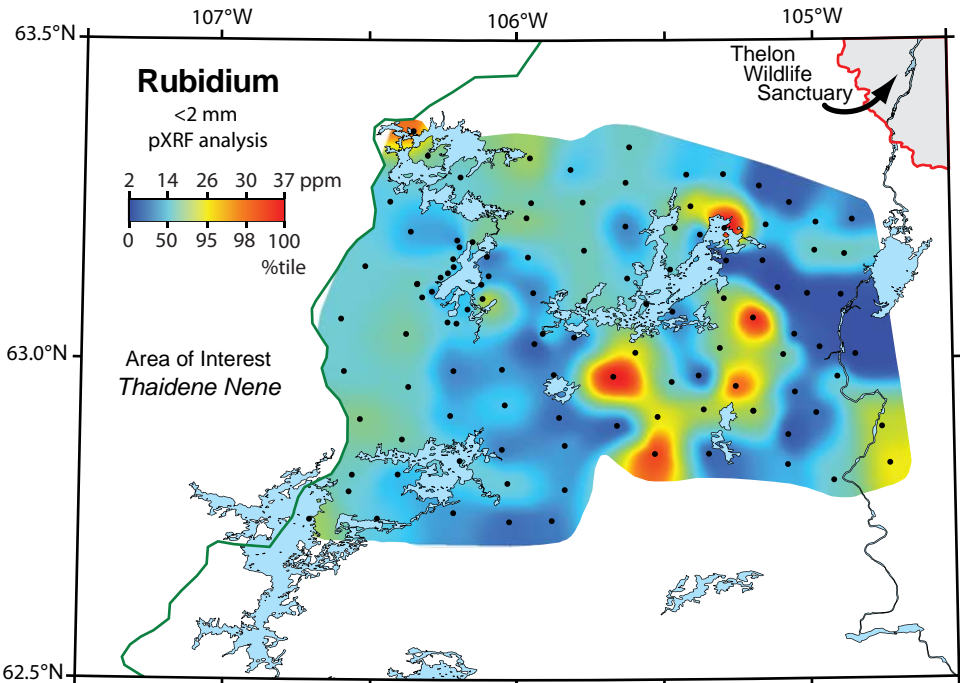


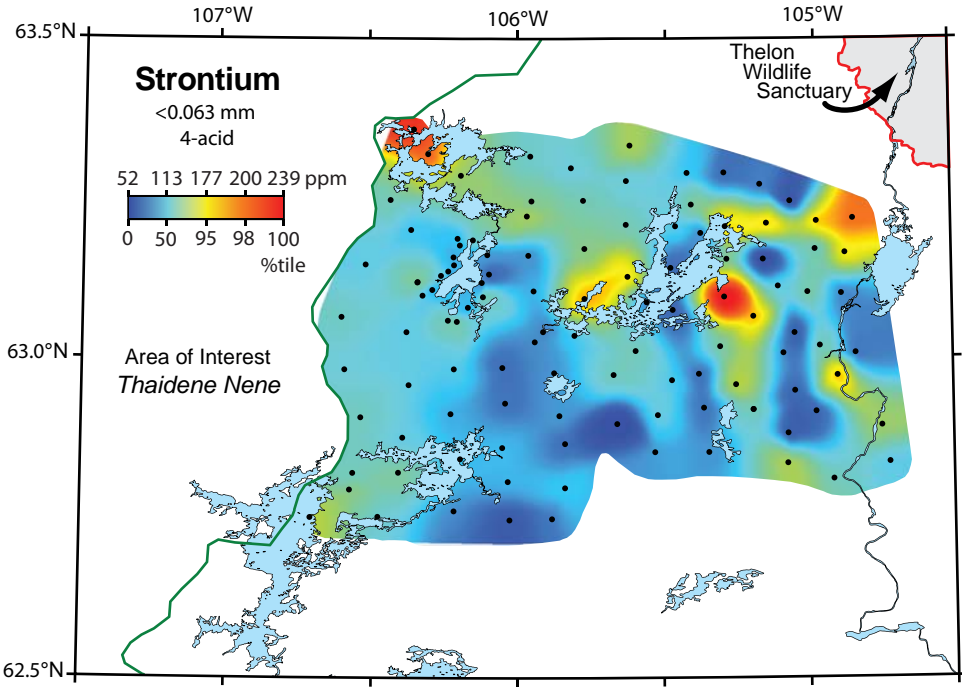
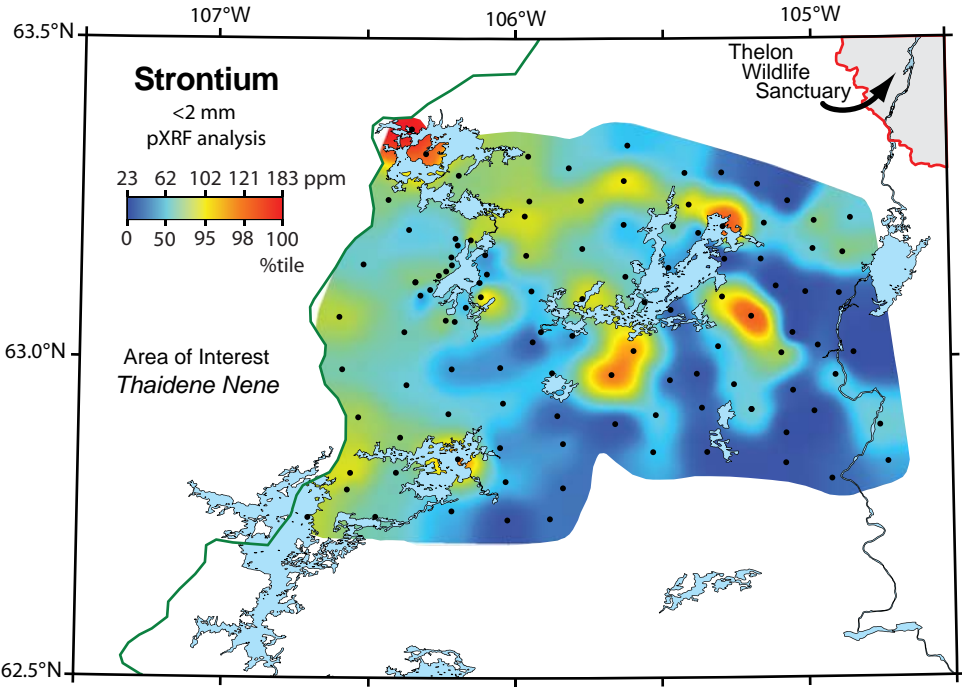












63.5°N 107°W 106°W 105°W
63.0°N
62.5°N

**No map generated
for aqua regia**

